Magnetism to Spintronics

Introduction to Solid State Physics
Kittel 8th ed
Chap. 11-13,

Condensed Matter Physics
Marder 2nd ed
Chap. 24-26,

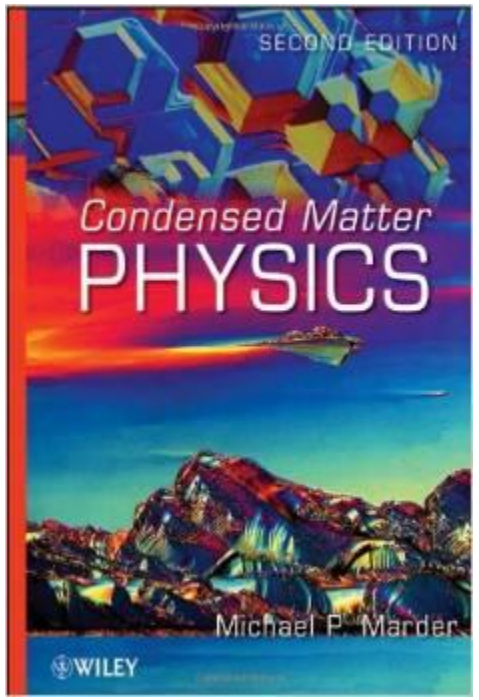

Why do most broken permanent magnets repel each other?

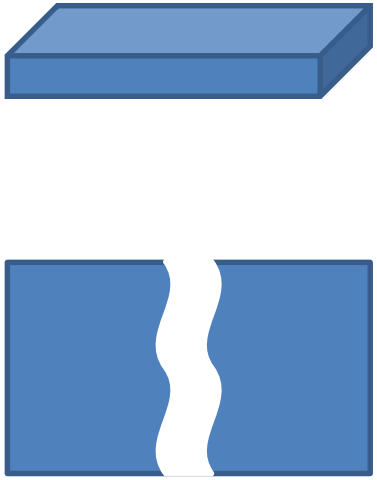

Cooperative phenomena

- Elementary excitations in solids describe the response of a solid to a perturbation
  - Quasiparticles

    usually fermions, resemble the particles that make the system, e.g. quasi-electrons
  - Collective excitations

    usually bosons, describe collective motions

    use second quantization with Fermi-Dirac or Bose-Einstein statistics

Magnetism

- the Bohr–van Leeuwen theorem

  when statistical mechanics and classical mechanics are applied consistently, the thermal average of the magnetization is always zero.
- Magnetism in solids is solely a quantum mechanical effect
- Origin of the magnetic moment:
  - Electron spin $\vec{S}$
  - Electron orbital momentum $\vec{L}$
- From (macroscopic) response to external magnetic field $\vec{H}$
  - Diamagnetism $\chi < 0$, $\chi \sim 1 \times 10^{-6}$, insensitive to temperature
  - Paramagnetism $\chi > 0$, $\chi = \frac{C}{T}$ Curie law

    $\chi = \frac{C}{T+\Delta}$ Curie-Weiss law
  - Ferromagnetism exchange interaction (quantum)

Magnetism

巨觀： 順磁性
Paramagnetism

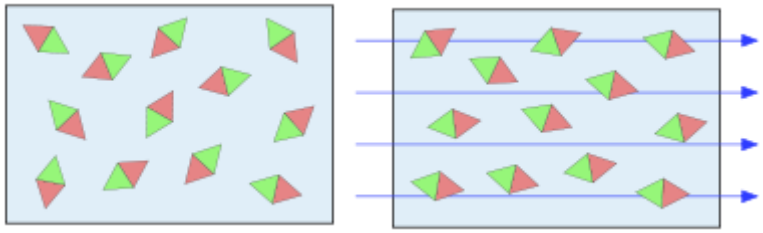

逆磁性
diamagnetism

微觀： 鐵磁性
Ferromagnetism

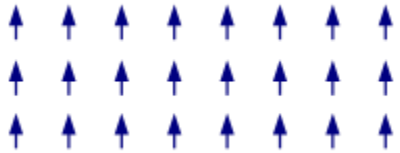

反鐵磁性
Antiferromagnetism

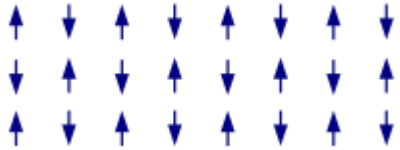

亞鐵磁性
Ferrimagnetism

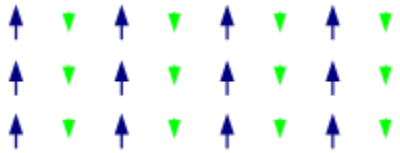

Family Tree of Magnetism

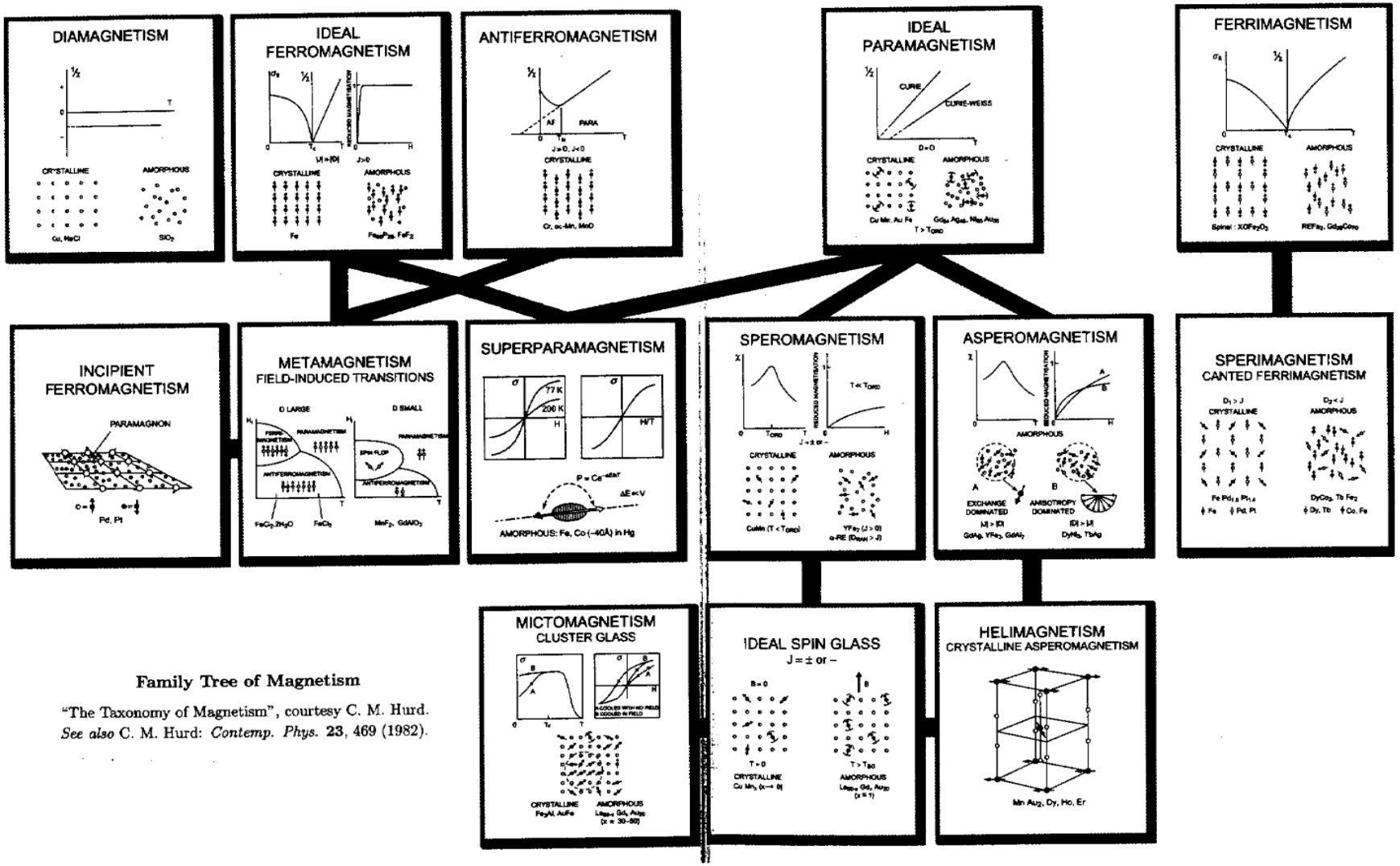

Family Tree of Magnetism

"The Taxonomy of Magnetism", courtesy C. M. Hurd.
See also C. M. Hurd: *Contemp. Phys.* **23**, 469 (1982).

Why do most broken permanent magnets repel each other?

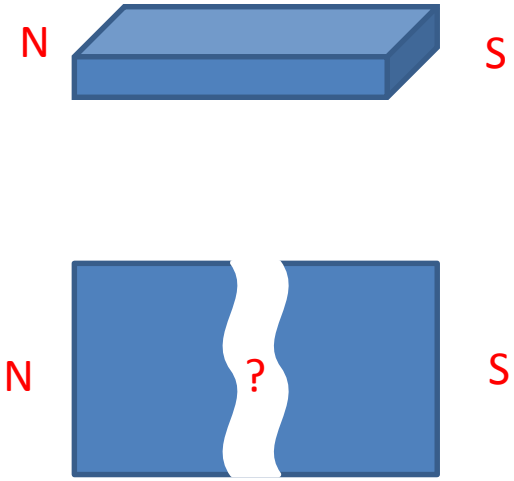

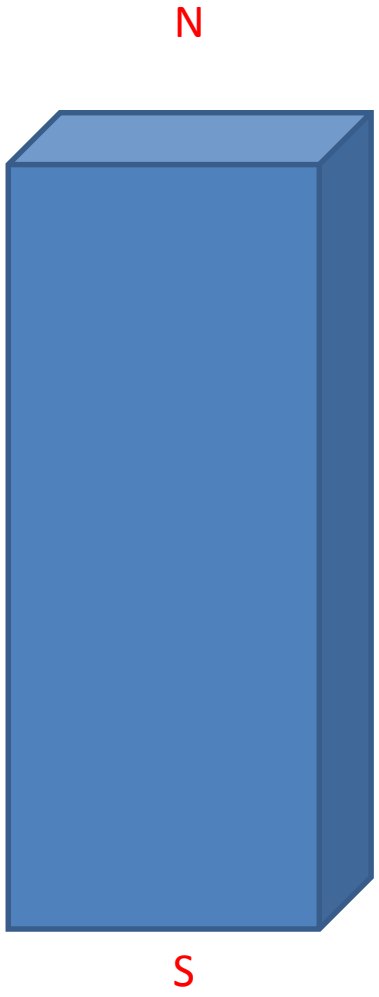

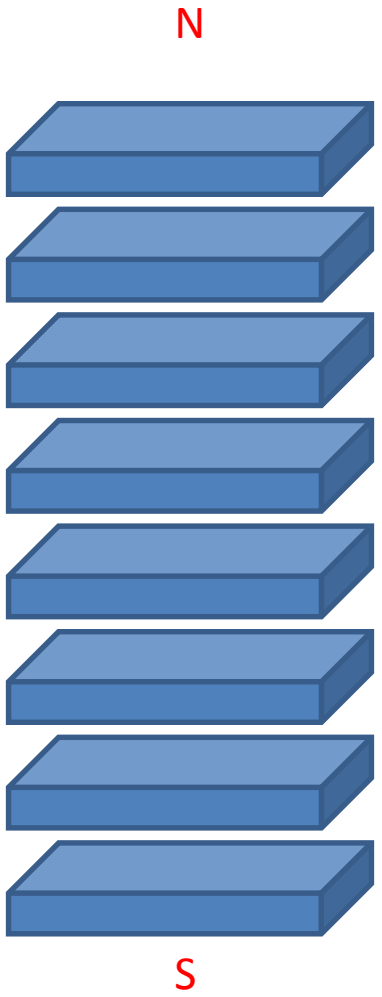

- Classical and quantum theory for diamagnetism
  - Calculate $\langle r^2 \rangle$
- Classical and quantum theory for paramagnetism
  - Superparamagnetism, Langevin function
  - Hund's rules
  - Magnetic state ${}^{2S+1}L_J$
  - Crystal field
  - Quenching of orbital angular momentum L_z
    - **Angular momentum operator**
    - **Spherical harmonics**
  - Jahn-Teller effect
  - Paramagnetic susceptibility of conduction electrons

- Ferromagnetism
  - Microscopic – ferro, antiferro, ferri magnetism
  - Exchange interaction
  - Exchange splitting – source of magnetization

    two-electron system spin-independent Schrodinger equation
  - Type of exchange: direct exchange, super exchange, indirect exchange, itinerant exchange
  - Spin Hamiltonian and Heisenberg model
  - Molecular-field (mean-field) approximation

Critical phenomena

Universality. Divergences near the critical point are identical in a variety of apparently different physical systems and also in a collection of simple models.
Scaling. The key to understanding the critical point lies in understanding the relationship between systems of different sizes. Formal development of this idea led to the *renormalization group* of Wilson (1975).

Landau Free Energy

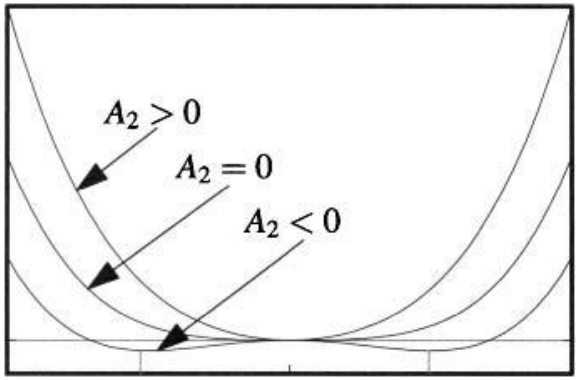

$$\mathcal{F}(M, T) = A_0(T) + A_2(T)M^2 + A_4(T)M^4 + HM.$$

$$t \equiv \frac{T - T_C}{T_C}$$

$$\mathcal{F} = a_2 t M^2 + a_4 M^4 + HM.$$

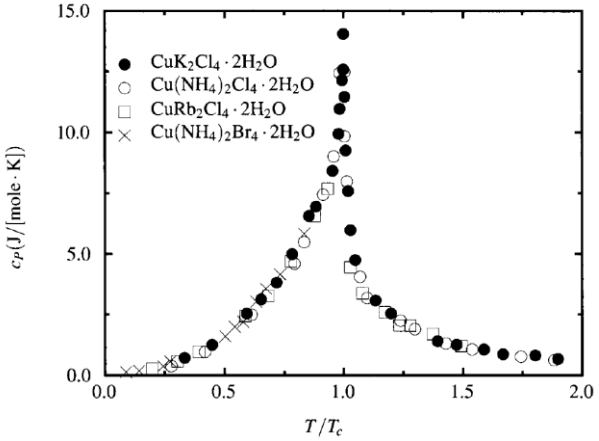

Molar heat capacities of four ferromagnetic copper salts versus scaled temperature T/T_c. [Source Jongh and Miedema (1974).]

Correspondence between Liquids and Magnets

- ***Specific Heat***— α
- ***Magnetization and Density***— β
- ***Compressibility and*** *Susceptibility*— γ
- ***Critical Isotherm***— δ
- ***Correlation Length*** — ν
- ***Power-Law Decay at Critical Point***— η

Summary of critical exponents, showing correspondence between fluid-gas systems, magnetic systems, and the three-dimensional Ising model.

Exponent	Fluid	Magnet	Mean Field Theory	Experiment	3d Ising
α	$C_V \sim \lvert t\rvert^{-\alpha}$	$C_V \sim \lvert t\rvert^{-\alpha}$	discontinuity	0.11–0.12	0.110
β	$\Delta n \sim \lvert t\rvert^{\beta}$	$M \sim \lvert t\rvert^{\beta}$	$\frac{1}{2}$	0.35–0.37	0.325
γ	$K_T \sim \lvert t\rvert^{-\gamma}$	$\chi \sim \lvert t\rvert^{-\gamma}$	1	1.21–1.35	1.241
δ	$P \sim \lvert \Delta n\rvert^{\delta}$	$\lvert H\rvert \sim \lvert M\rvert^{\delta}$	3	4.0–4.6	4.82
ν	$\xi \sim \lvert t\rvert^{-\nu}$	$\xi \sim \lvert t\rvert^{-\nu}$		0.61–0.64	0.63
η	$g(r) \sim r^{-1-\eta}$	$g(r) \sim r^{-1-\eta}$		0.02–0.06	0.032

Source: Vicentini-Missoni (1972) p. 67, Cummins (1971), p. 417, and Goldenfeld (1992) p. 384.

Relations Among Exponents

$$\alpha + 2\beta + \gamma = 2 \qquad (2-\eta)\nu = \gamma$$

$$\delta = 1 + \frac{\gamma}{\beta} \qquad 2 - \alpha = 3\nu$$

- Stoner band ferromagnetism

  Teodorescu, C. M.; Lungu, G. A. (November 2008). "Band ferromagnetism in systems of variable dimensionality". *Journal of Optoelectronics and Advanced Materials* **10** (11): 3058–3068.

$$\mathcal{E} = \int_0^{\mathcal{E}_F-\Delta} d\mathcal{E}'\, D(\mathcal{E}')\mathcal{E}' + \frac{1}{2}\int_{\mathcal{E}_F-\Delta}^{\mathcal{E}_F+\Delta} d\mathcal{E}'\, D(\mathcal{E}')\mathcal{E}' - \frac{1}{2}nJ\,\langle S\rangle^2$$

$$\langle S\rangle = \frac{1}{2n}\int_{\mathcal{E}_F-\Delta}^{\mathcal{E}_F+\Delta} d\mathcal{E}'\,\frac{1}{2}D(\mathcal{E}') = \frac{1}{2n}D(\mathcal{E}_F)\Delta$$

$$\left.\frac{\partial\mathcal{E}}{\partial\Delta}\right|_{\mathcal{E}_F} = \Delta D(\mathcal{E}_F) - \frac{J}{4n}D(\mathcal{E}_F)^2\Delta$$

$$\left.\frac{\partial\mathcal{E}}{\partial\Delta}\right|_{\mathcal{E}_F} = 0 \Rightarrow \frac{J}{n}D(\mathcal{E}_F) = 4$$

Ferromagnetic elements: 鐵 Fe, 鈷 Co, 鎳 Ni, 釓 Gd, 鏑 Dy,
錳 Mn, 鈀 Pd ??

Elements with ferromagnetic properties

合金, alloys

錳氧化物 MnOx, ……

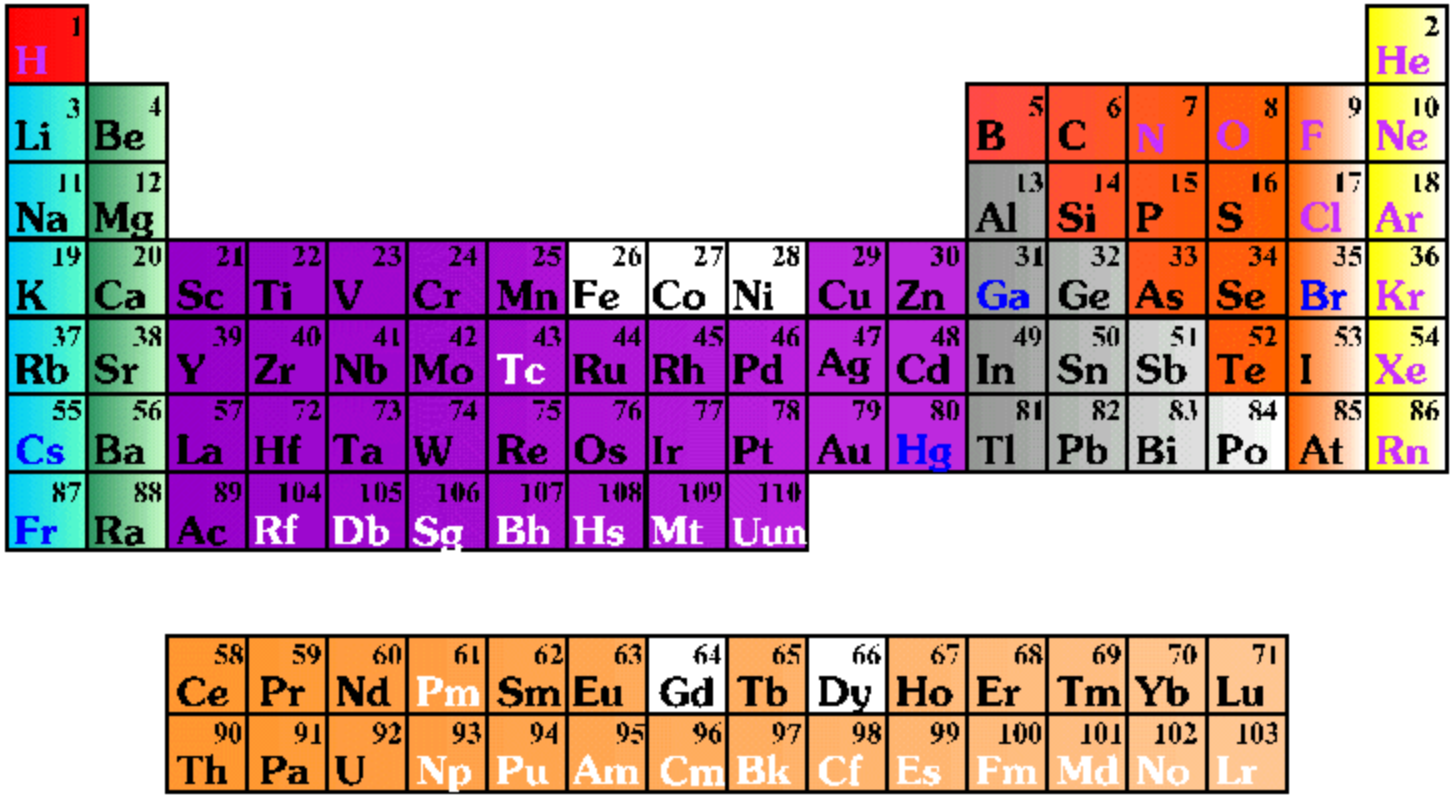

Platonic solid

From Wikipedia

In geometry, a Platonic solid is a convex polyhedron that is regular, in the sense of a regular polygon. Specifically, the faces of a Platonic solid are congruent regular polygons, with the same number of faces meeting at each vertex; thus, all its edges are congruent, as are its vertices and angles. There are precisely five Platonic solids (shown below):

The name of each figure is derived from its number of faces: respectively 4, 6, 8, 12, and 20.

The aesthetic beauty and symmetry of the Platonic solids have made them a favorite subject of geometers for thousands of years. They are named for the ancient Greek philosopher Plato who theorized that the classical elements were constructed from the regular solids.

				
Tetrahedron	Cube hexahedron	Octahedron	Dodecahedron	Icosahedron

Solar system

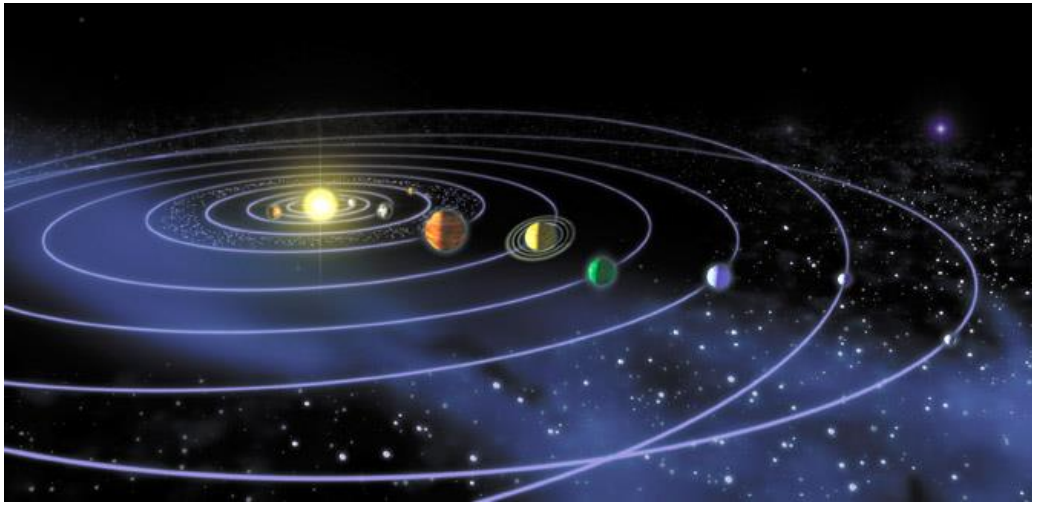

Electronic orbit

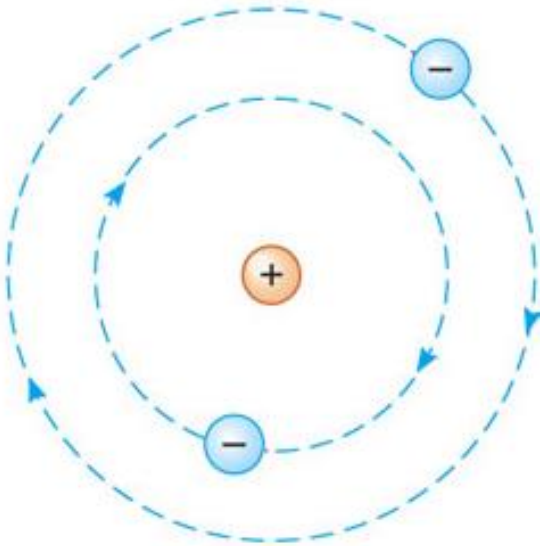

s, p electron orbits

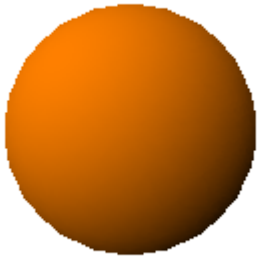

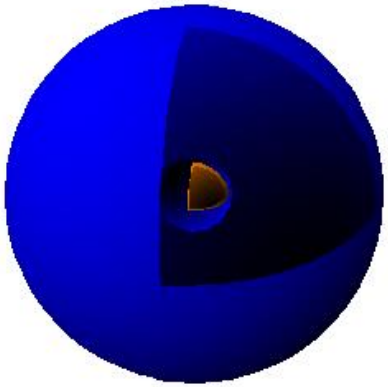

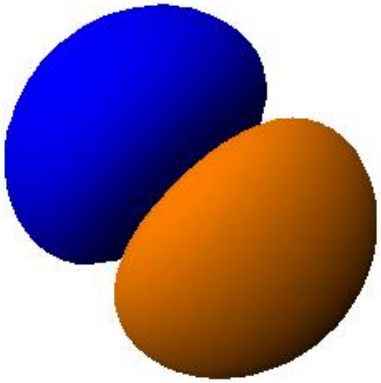

Orbital viewer

Resonance

One-dimensional

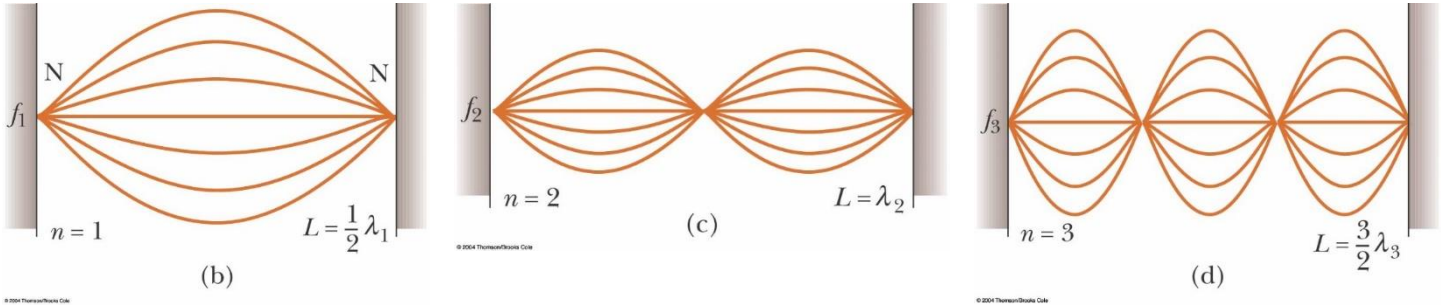

Two-dimensional

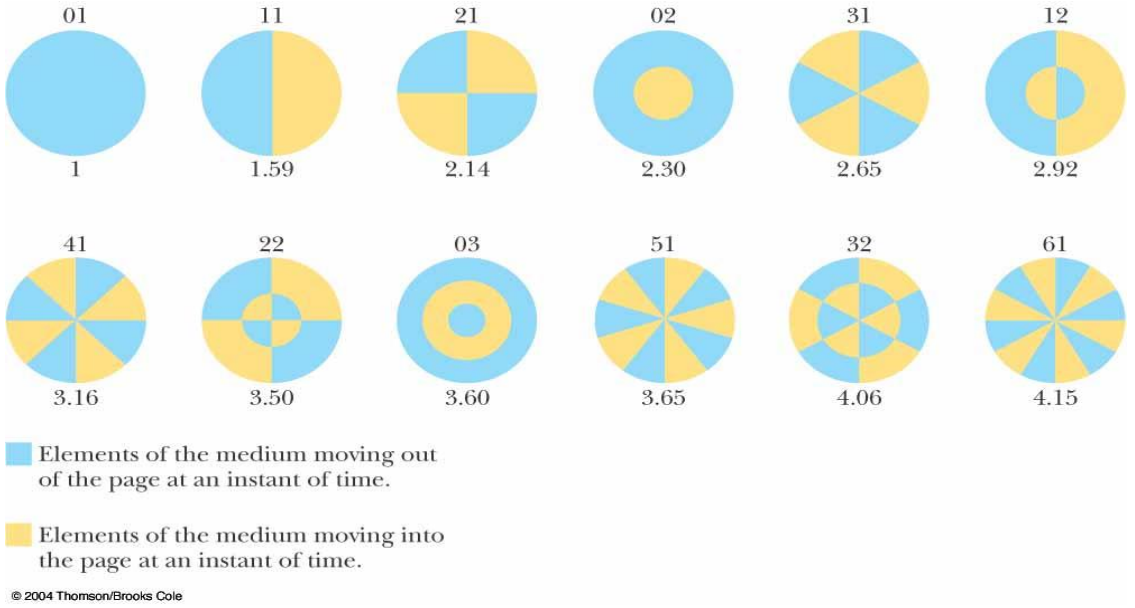

Three-dimensional

Hydrogen atom

3d transition metals:

Mn atom has 5 d ↑ electrons Bulk Mn is NOT magnetic

s, p electron orbital

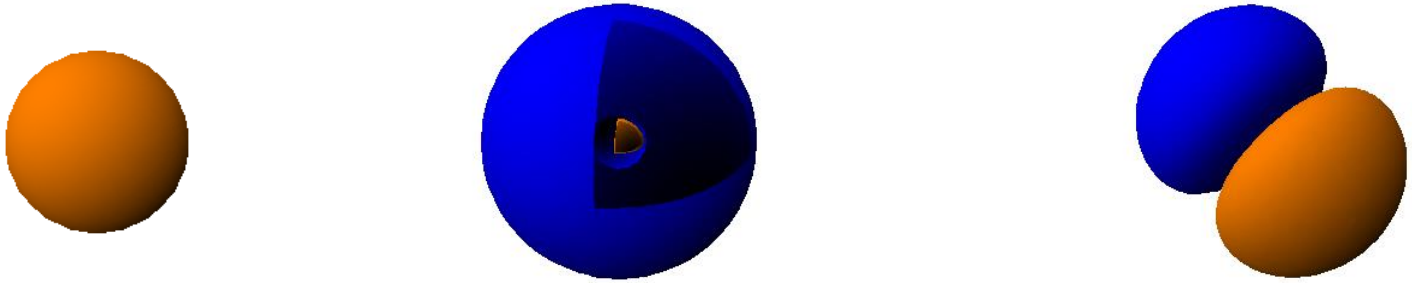

3d electron distribution in real space

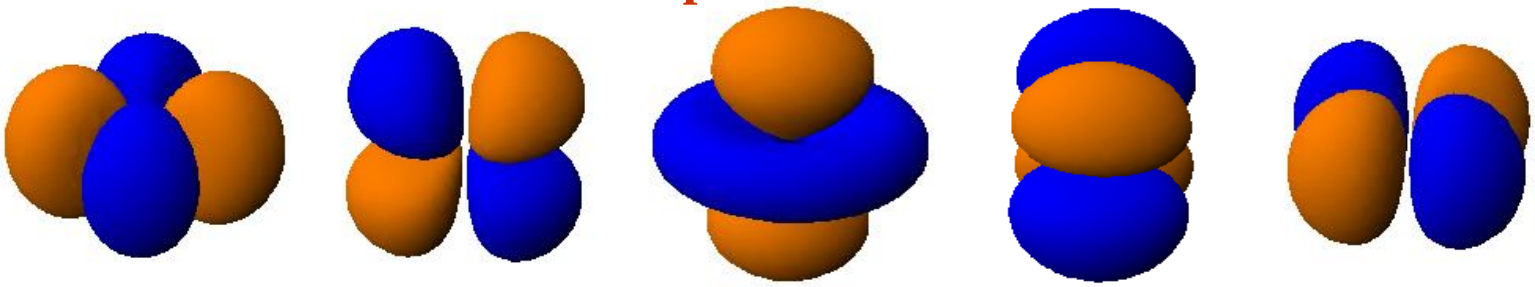

Co atom has 5 d ↑electrons and 2 d ↓ electrons

Bulk Co is magnetic.

Orbital viewer

d orbitals

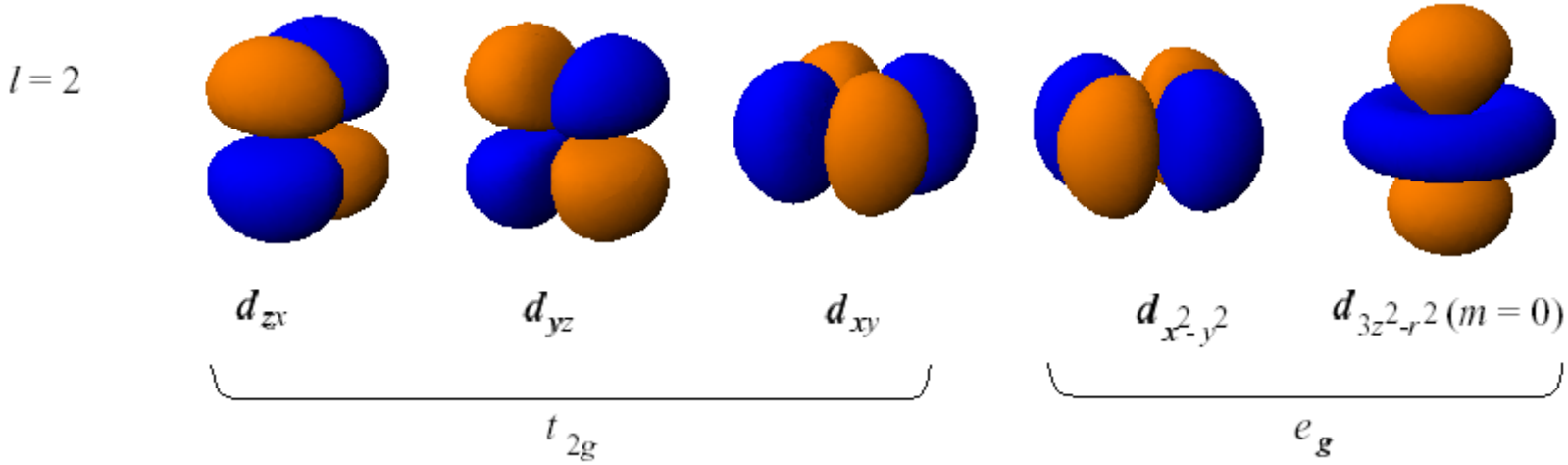

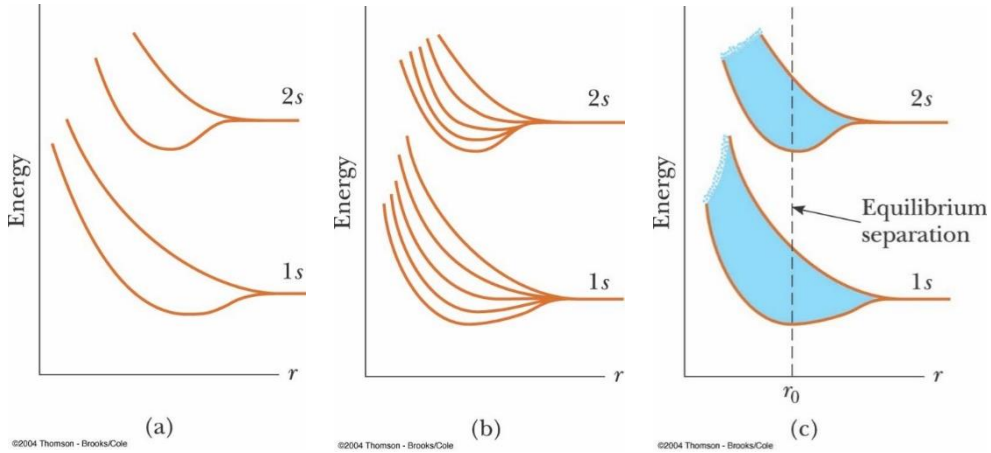

Crystal-field splitting

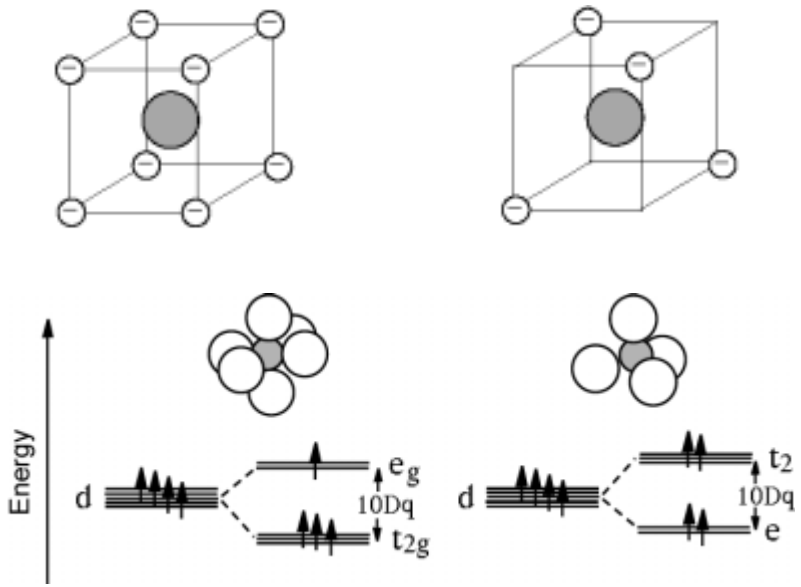

Stern-Gerlach Experiment

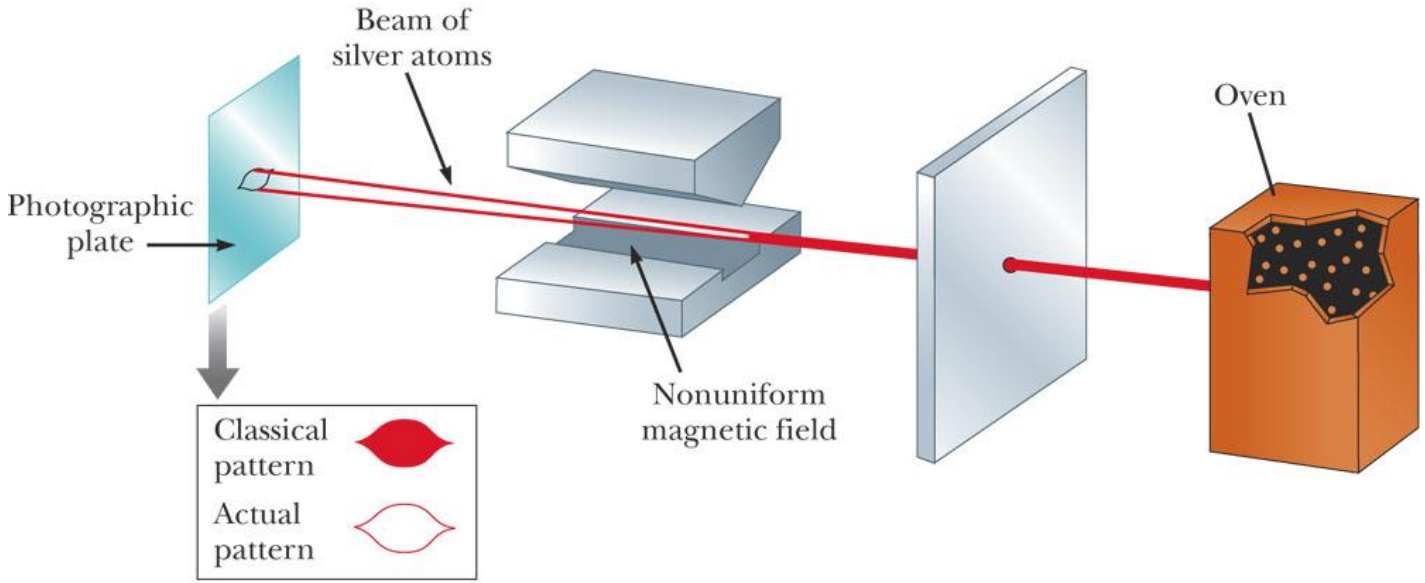

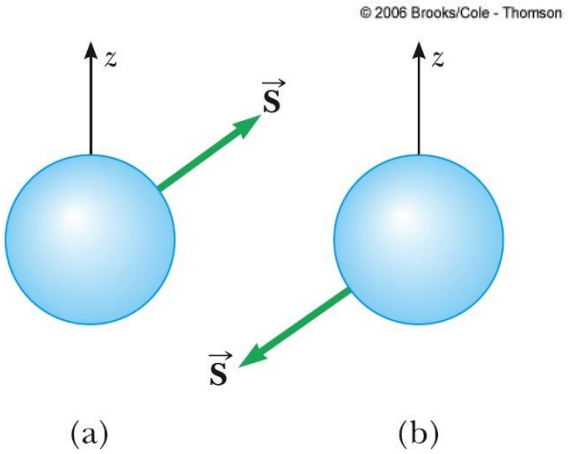

There are two kinds of electrons: spin-up and spin-down.

Stoner criterion for ferromagnetism:

I $N(E_F) > 1$, I is the **Stoner exchange parameter** and $N(E_F)$ is the density of states at the Fermi energy.

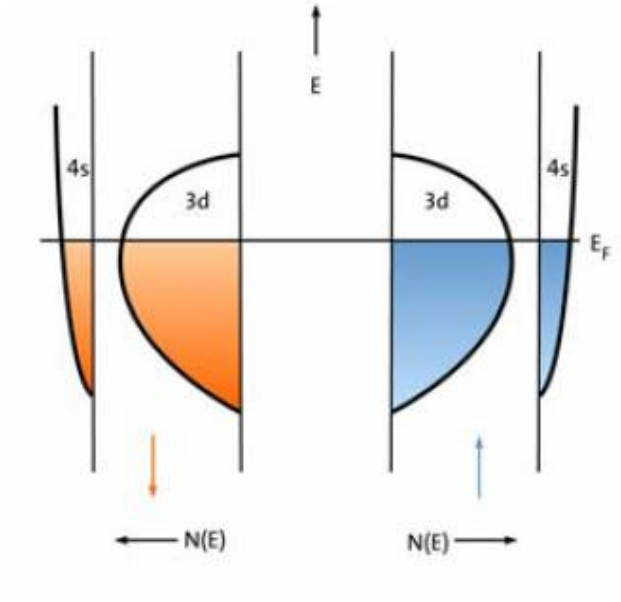

For the non-magnetic state there are identical density of states for the two spins.

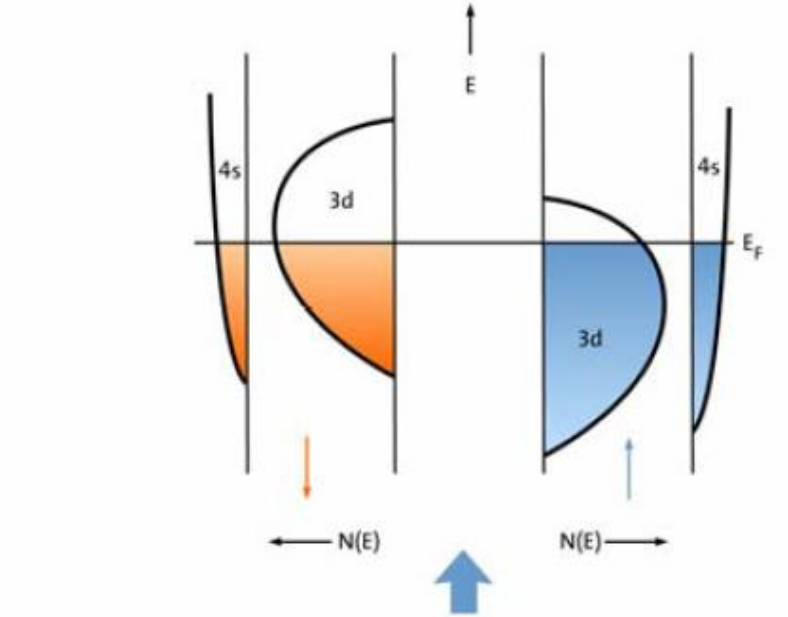

For a ferromagnetic state, N↑ > N↓. The polarization is indicated by the thick blue arrow.

Schematic plot for the energy band structure of 3d transition metals.

Teodorescu and Lungu, "Band ferromagnetism in systems of variable dimensionality". *J Optoelectronics and Adv. Mat.* **10,** 3058–3068 (2008).

Exchange interaction

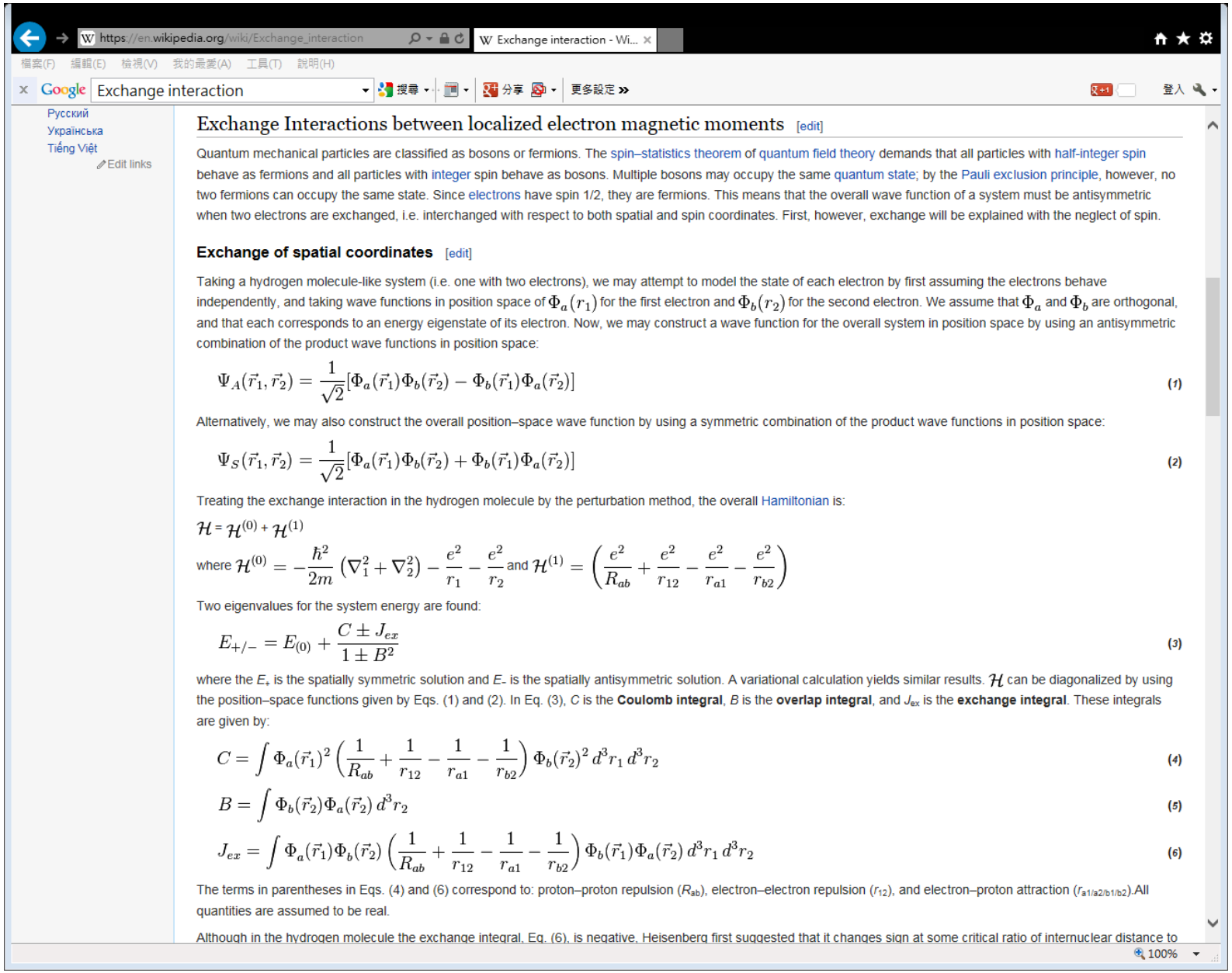

Berry Phase

Aharonov-Bohm Effect

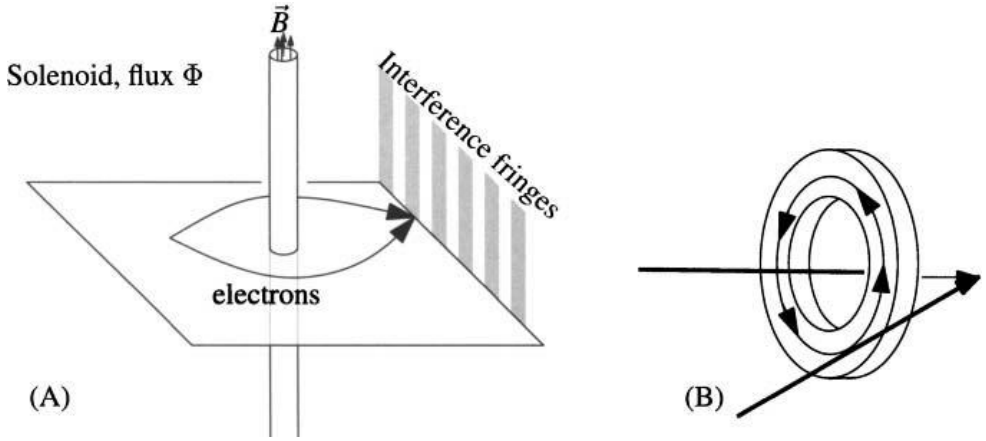

Electrons traveling around a flux tube suffer a phase change and can interfere with themselves even if they only travel through regions where B = 0.
(B) An open flux tube is not experimentally realizable, but a small toroidal magnet with no flux leakage can be constructed instead.

$$\Phi = \int d^2r\, B_z = \oint d\vec{r} \cdot \vec{A}$$

$$A_\phi = \frac{\Phi}{2\pi r}$$

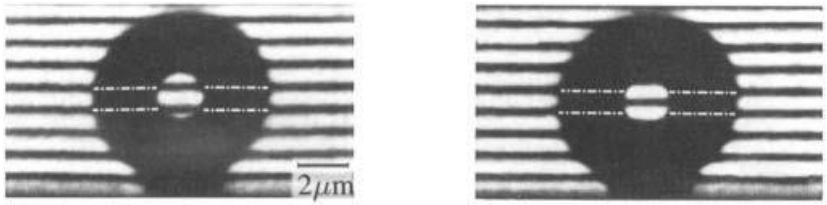

Electron hologram showing interference fringes of electrons passing through small toroidal magnet. The magnetic flux passing through the torus is quantized so as to produce an integer multiple of π phase change in the electron wave functions. The electron is completely screened from the magnetic induction in the magnet. In (A) the phase change is 0, while in (B) the phase change is π.
[Source: Tonomura (1993), p. 67.]

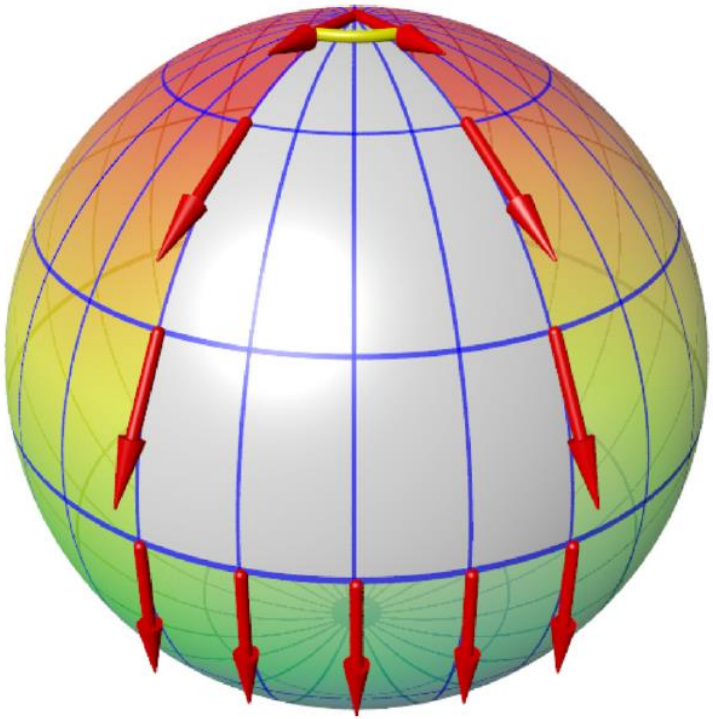

Parallel transport of a vector along a closed path on the sphere S_2 leads to a geometric phase between initial and final state.

Real-space Berry phases: Skyrmion soccer (invited)
Karin Everschor-Sitte and Matthias Sitte
Journal of Applied Physics **115**, 172602 (2014); doi: 10.1063/1.4870695

Berry phase formalism for intrinsic Hall effects

From Prof. Guo Guang-Yu

Berry phase

[Berry, Proc. Roy. Soc. London A 392, 451 (1984)]

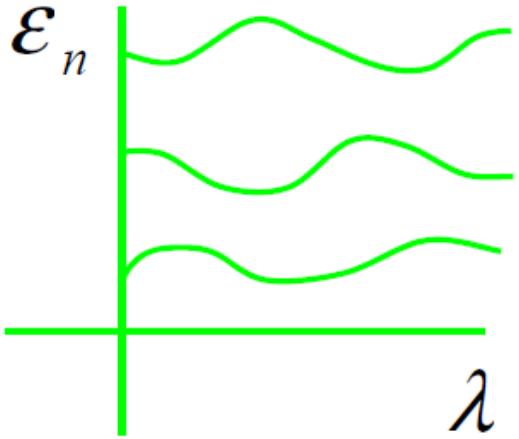

Parameter dependent system:

$$\{\varepsilon_n(\lambda),\ \psi_n(\lambda)\}$$

Adiabatic theorem:

$$\Psi(t) = \psi_n(\lambda(t))\ e^{-i\int_0^t dt\,\varepsilon_n/\hbar}\ e^{-i\gamma_n(t)}$$

Geometric phase:

$$\gamma_n = \int_{\lambda_0}^{\lambda_t} d\lambda \left\langle \psi_n \middle| i\frac{\partial}{\partial\lambda} \middle| \psi_n \right\rangle$$

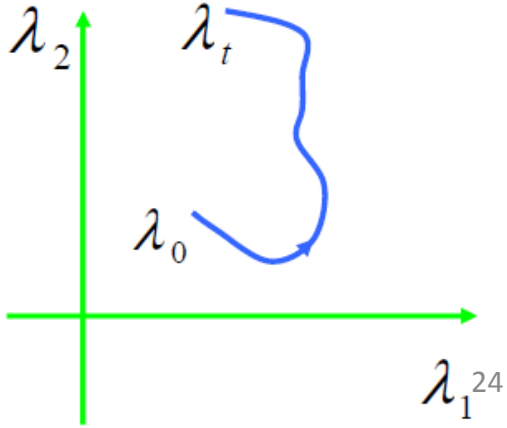

Well defined for a closed path

From Prof. Guo Guang-Yu

$$\gamma_n = \oint_C d\lambda \langle \psi_n | i \frac{\partial}{\partial \lambda} | \psi_n \rangle$$

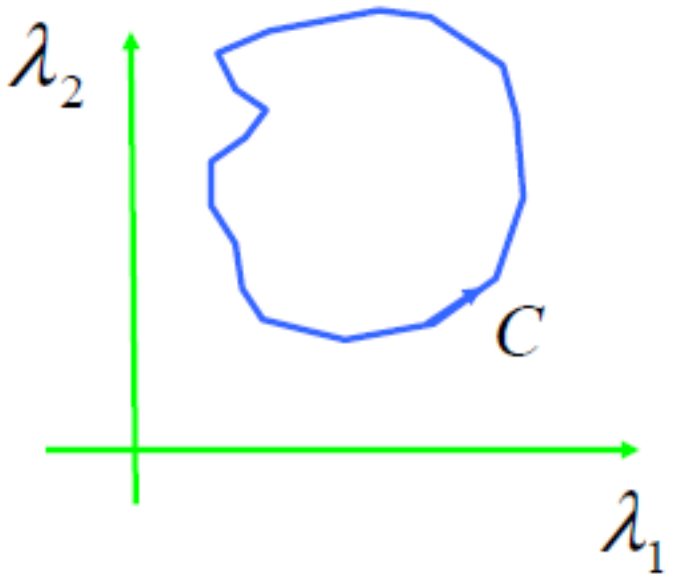

Stokes theorem

$$\gamma_n = \iint d\lambda_1 d\lambda_2 \, \Omega$$

Berry Curvature

$$\Omega = i \frac{\partial}{\partial \lambda_1} \langle \psi | \frac{\partial}{\partial \lambda_2} | \psi \rangle - i \frac{\partial}{\partial \lambda_2} \langle \psi | \frac{\partial}{\partial \lambda_1} | \psi \rangle$$

Analogies

From Prof. Guo Guang-Yu

Berry curvature

$$\Omega(\vec{\lambda})$$

Magnetic field

$$B(\vec{r})$$

Berry connection

$$\langle \psi | i \frac{\partial}{\partial \lambda} | \psi \rangle$$

Vector potential

$$A(\vec{r})$$

Geometric phase

$$\oint d\lambda \langle \psi | i \frac{\partial}{\partial \lambda} | \psi \rangle = \iint d^2\lambda \ \Omega(\vec{\lambda})$$

Aharonov-Bohm phase

$$\oint dr \ A(\vec{r}) = \iint d^2 r \ B(\vec{r})$$

Chern number

$$\oiint d^2\lambda \ \Omega(\vec{\lambda}) = \text{integer}$$

Dirac monopole

$$\oiint d^2 r \ B(\vec{r}) = \text{integer} \ h/e$$

Semiclassical dynamics of Bloch electrons

From Prof. Guo Guang-Yu

Old version [e.g., Aschroft, Mermin, 1976]

$$\dot{\mathbf{x}}_c = \frac{1}{\hbar}\frac{\partial \varepsilon_n(\mathbf{k})}{\partial \mathbf{k}},$$

$$\dot{\mathbf{k}} = -\frac{e}{\hbar}\mathbf{E} - \frac{e}{\hbar}\dot{\mathbf{x}}_c \times \mathbf{B} = \frac{e}{\hbar}\frac{\partial \varphi(\mathbf{r})}{\partial \mathbf{r}} - \frac{e}{\hbar}\dot{\mathbf{x}}_c \times \mathbf{B}$$

New version [Marder, 2000]

Berry phase correction [Chang & Niu, PRL (1995), PRB (1996)]

$$\dot{\mathbf{x}}_c = \frac{1}{\hbar}\frac{\partial \varepsilon_n(\mathbf{k})}{\partial \mathbf{k}} - \dot{\mathbf{k}} \times \boldsymbol{\Omega}_n(\mathbf{k}),$$

$$\dot{\mathbf{k}} = \frac{e}{\hbar}\frac{\partial \varphi(\mathbf{r})}{\partial \mathbf{r}} - \frac{e}{\hbar}\dot{\mathbf{x}}_c \times \mathbf{B},$$

$$\boldsymbol{\Omega}_n(\mathbf{k}) = -\mathrm{Im}\left\langle \frac{\partial u_{n\mathbf{k}}}{\partial \mathbf{k}} \middle| \times \middle| \frac{\partial u_{n\mathbf{k}}}{\partial \mathbf{k}} \right\rangle$$

(Berry curvature)

Demagnetization factor D

can be solved analytically in some cases, numerically in others

For an ellipsoid $D_x + D_y + D_z = 1$ (SI units) $D_x + D_y + D_z = 4\pi$ (cgs units)

Solution for Spheroid $a = b \neq c$

1. Prolate spheroid (football shape) $c/a = r > 1$; $a = b$, In cgs units

$$D_c = \frac{4\pi}{r^2-1}\left[\frac{r}{\sqrt{r^2-1}}\ln\left(r+\sqrt{r^2-1}\right)-1\right]$$

$$D_a = D_b = \frac{4\pi - D_c}{2}$$

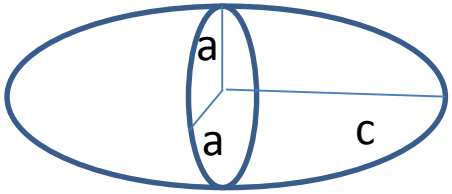

Limiting case r >> 1 (long rod)

$$D_c = \frac{4\pi}{r^2}[\ln(2r)-1] \ll 1$$

$$D_a = D_b = 2\pi$$

Note: you measure 2πM *without* knowing the sample

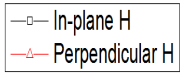

2. Oblate Spheroid (pancake shape) $c/a = r < 1$; $a = b$

$$D_c = \frac{4\pi}{1-r^2}\left[1-\frac{r}{\sqrt{1-r^2}}\cos^{-1} r\right]$$

$$D_a = D_b = \frac{4\pi - D_c}{2}$$

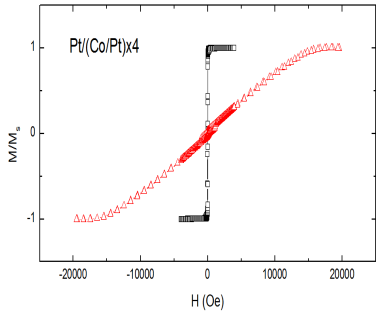

Limiting case r >> 1 (flat disk)

$$D_c = 4\pi$$

$$D_a = D_b = \pi^2 r \ll 1$$

Note: you measure 4πM *without* knowing the sample

Surface anisotropy

$$E = E_{exchange} + E_{Zeeman} + E_{mag} + E_{anisotropy} + \cdots$$

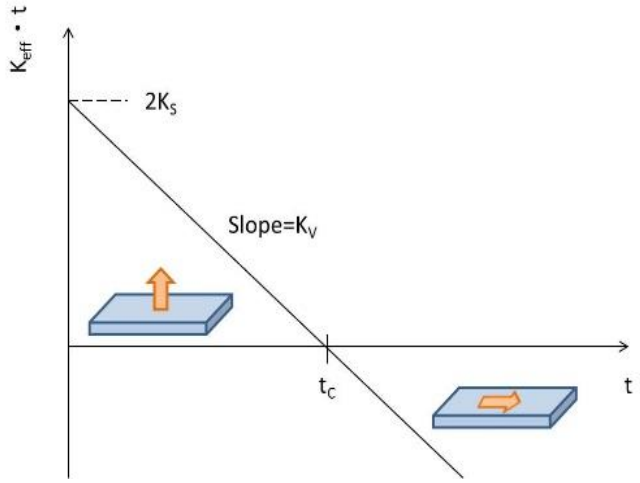

- $E_{ex} : \sum 2J\overrightarrow{S_i} \cdot \overrightarrow{S_j}$
- $E_{Zeeman} : \vec{M} \cdot \vec{H}$
- $E_{mag} : \frac{1}{8\pi} \int B^2 dV$
- $E_{anisotropy}$

For hcp Co= $K_1' \sin^2\theta + K_2' \sin^4\theta$

For bcc Fe = $K_1(\alpha_1^2\alpha_2^2 + \alpha_2^2\alpha_3^2 + \alpha_3^2\alpha_1^2) + K_2(\alpha_1^2\alpha_2^2\alpha_3^2)$

α_i : directional cosines

Surface anisotropy $K_{\text{eff}} = \frac{2K_S}{t} + K_V$ ➔ $K_{\text{eff}} \cdot t = 2K_S + K_V \cdot t$

Stoner–Wohlfarth model

A widely used model for the magnetization of single-domain ferromagnets. It is a simple example of magnetic hysteresis and is useful for modeling small magnetic particles

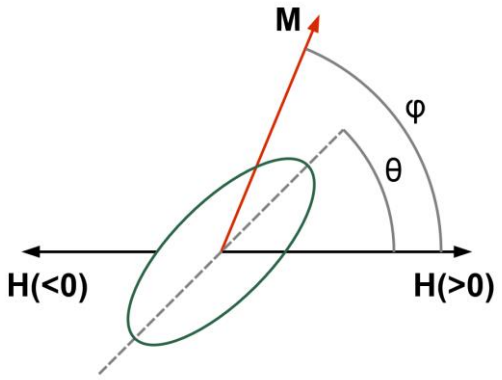

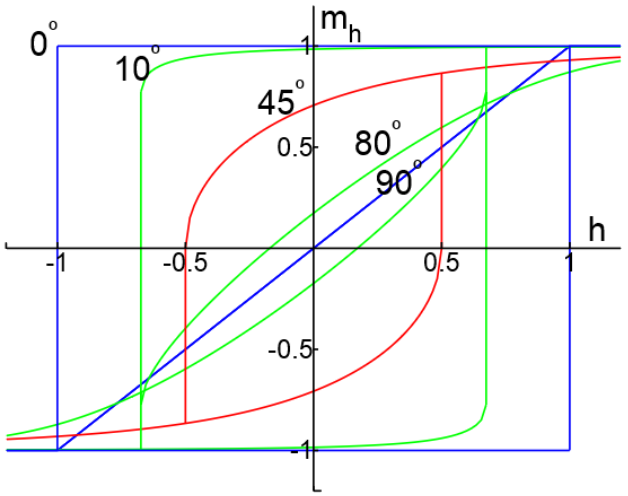

$$E = K_u V \sin^2(\phi - \theta) - \mu_0 M_s V H \cos\phi,$$

where K_u is the uniaxial anisotropy parameter, V is the volume of the magnet, M_s is the saturation magnetization.

Ferromagnetic domains

- competition between exchange, anisotropy, and magnetic energies.
- Bloch wall: rotation out of the plane of the two spins
- Neel wall: rotation within the plane of the two spins

For a 180° Bloch wall rotated in N+1 atomic planes $N\Delta E_{ex} = N(JS^2\left(\frac{\pi}{N}\right)^2)$

Wall energy density $\sigma_w = \sigma_{ex} + \sigma_{anis} \approx JS^2\pi^2/(Na^2) + KNa$ a : lattice constant

$\partial\sigma_w/\partial N \equiv 0,$ $N = \sqrt{[JS^2\pi^2/(Ka^3)]} \approx 300$ in Fe

$\sigma_w = 2\pi\sqrt{KJS^2/a} \approx$ 1 erg/cm^2 in Fe

Wall width $Na = \pi\sqrt{JS^2/Ka} \equiv \pi\sqrt{\frac{A}{K}}$, $A = JS^2/a$ Exchange stiffness constant

Domain wall energy γ versus thickness D of $Ni_{80}Fe_{20}$ thin films

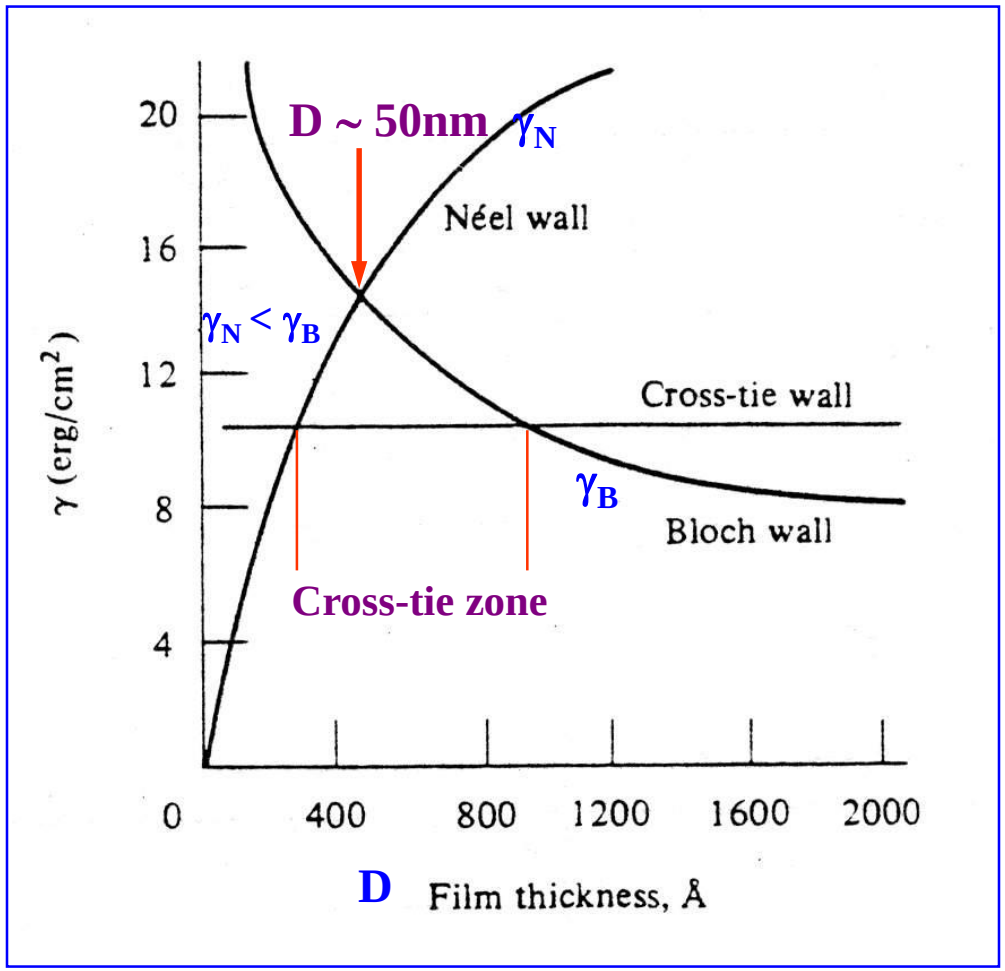

$\gamma_N < \gamma_B \sim 50nm$

Thick films have Bloch walls
Thin films have Neel walls

Cross-tie walls show up in between.

$A=10^{-6}$ erg/cm

$K=1500$ erg/cm^3

Magnetic Resonance

- Nuclear Magnetic Resonance (NMR)
  - Line width
  - Hyperfine Splitting, Knight Shift
  - Nuclear Quadrupole Resonance (NQR)
- Ferromagnetic Resonance (FMR)
  - Shape Effect
  - Spin Wave resonance (SWR)
- Antiferromagnetic Resonance (AFMR)
- Electron Paramagnetic Resonance (EPR or ESR)
  - Exchange narrowing
  - Zero-field Splitting
- Maser

What we can learn:

- From absorption fine structure ➔ electronic structure of single defects
- From changes in linewidth ➔ relative motion of the spin to the surroundings
- From resonance frequency ➔ internal magnetic field
- Collective spin excitations

FMR

Equation of motion of a magnetic moment $\boldsymbol{\mu}$ in an external field B_0

$$\frac{\hbar d\boldsymbol{I}}{dt} = \boldsymbol{\mu} \times \boldsymbol{B} \qquad \boldsymbol{\mu} = \gamma\hbar\boldsymbol{I} \qquad \frac{d\boldsymbol{\mu}}{dt} = \gamma\boldsymbol{\mu} \times \boldsymbol{B} \qquad \frac{d\boldsymbol{M}}{dt} = \gamma\boldsymbol{M} \times \boldsymbol{B}$$

Landau-Lifshitz-Gilbert (LLG) equation

$$\frac{d\boldsymbol{M}}{dt} = -\gamma\boldsymbol{M} \times \boldsymbol{H}_{\text{eff}} + \alpha\boldsymbol{M} \times \frac{d\boldsymbol{M}}{dt}$$

Shape effect:

internal magnetic field

$$B_x^i = B_x^0 - N_x M_x \qquad B_y^i = B_y^0 - N_y M_y \qquad B_z^i = B_z^0 - N_z M_z$$

$$\frac{dM_x}{dt} = \gamma\left(M_y B_z^i - M_z B_y^i\right) = \gamma[B_0 + \left(N_y - N_z\right)M]M_y$$

$$\frac{dM_y}{dt} = \gamma[M(-N_x M_x) - M_x(B_0 - N_z M)] = -\gamma[B_0 + (N_x - N_z)M]M_x$$

To first order $\frac{dM_z}{dt} = 0$ $M_z = M$

$$\begin{vmatrix} i\omega & \gamma[B_0 + \left(N_y - N_z\right)M] \\ -\gamma[B_0 + (N_x - N_z)M] & i\omega \end{vmatrix} = 0$$

$$\omega_0^2 = \gamma^2[B_0 + \left(N_y - N_z\right)M][B_0 + (N_x - N_z)M]$$

Uniform mode

Uniform mode

Sphere flat plate with perpendicular field flat plate with in-plane field

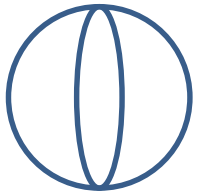

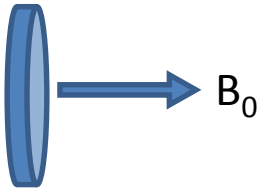

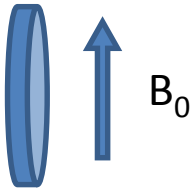

$N_x = N_y = N_z$ $\quad \omega_0 = \gamma\, B_0$

$N_x = N_y = 0 \quad N_z = 4\pi$ $\quad \omega_0 = \gamma\,(B_0 - 4\pi M)$

$N_x = N_z = 0 \quad N_y = 4\pi$ $\quad \omega_0 = \gamma\,[B_0(B_0 + 4\pi M)]^{1/2}$

Spin wave resonance; Magnons

Consider a one-dimensional spin chain with only nearest-neighbor interactions.

$U = -2J \sum \vec{S_i} \cdot \vec{S_j}$ We can derive $\hbar\omega = 4JS(1 - \cos ka)$

When $ka \ll 1$ $\quad \hbar\omega \cong (2JSa^2)k^2$

flat plate with perpendicular field $\quad \omega_0 = \gamma\,(B_0 - 4\pi M) + Dk^2$

Quantization of (uniform mode) spin waves, then consider the thermal excitation of Mannons, leads to Bloch $T^{3/2}$ law. $\quad \Delta M/M(0) \propto T^{3/2}$

AFMR

Spin wave resonance; Antiferromagnetic Magnons

Consider a one-dimensional antiferromangetic spin chain with only nearest-neighbor interactions. Treat sublattice A with up spin S and sublattice B with down spin –S, J<0.

$U = -2J \sum \overrightarrow{S_i} \cdot \overrightarrow{S_j}$ We can derive $\hbar\omega = -4JS|\sin ka|$

When $ka << 1$ $\hbar\omega \cong (-4JS)|ka|$

AFMR

exchange plus anisotropy fields on the two sublattices

$\boldsymbol{B}_1 = -\lambda \boldsymbol{M}_2 + B_A \hat{\boldsymbol{z}}$ on $\mathbf{M}_1$ $\boldsymbol{B}_2 = -\lambda \boldsymbol{M}_1 - B_A \hat{\boldsymbol{z}}$ on $\mathbf{M}_2$

$M_1^z \equiv M$ $M_2^z \equiv -M$ $M_1^+ \equiv M_1^x + iM_1^y$ $M_2^+ \equiv M_2^x + iM_2^y$ $B_E \equiv \lambda M$

$$\frac{dM_1^+}{dt} = -i\gamma[M_1^+(B_A + B_E) + M_2^+ B_E]$$

$$\frac{dM_2^+}{dt} = -i\gamma[M_2^+(B_A + B_E) + M_1^+ B_E]$$

$$\begin{vmatrix} \gamma(B_A + B_E) - \omega & \gamma B_E \\ B_E & \gamma(B_A + B_E) + \omega \end{vmatrix} = 0$$

$\omega_0^2 = \gamma^2 B_A(B_A + 2B_E)$ Uniform mode

Spintronics

Electronics with electron spin as an extra degree of freedom
Generate, inject, process, and detect spin currents

- Generation: ferromagnetic materials, spin Hall effect, spin pumping effect etc.
- Injection: interfaces, heterogeneous structures, tunnel junctions
- Process: spin transfer torque
- Detection: Giant Magnetoresistance, Tunneling MR
- Historically, from magnetic coupling to transport phenomena

  important materials: CoFe, CoFeB, Cu, Ru, IrMn, PtMn, MgO, Al2O3, Pt, Ta

RKKY (*Ruderman-Kittel-Kasuya-Yosida*) interaction

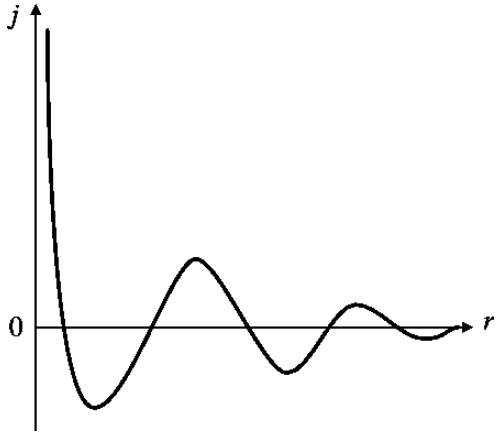

coupling coefficient

$$j\left(\boldsymbol{R}_i-\boldsymbol{R}_{i'}\right)=9\pi\left(\frac{j^2}{\epsilon_F}\right)F\left(2k_F|\boldsymbol{R}_i-\boldsymbol{R}_{i'}|\right)$$

$$F(x)=\frac{x\cos x-\sin x}{x^4}$$

Magnetic coupling in superlattices

- Long-range incommensurate magnetic order in a Dy-Y multilayer

M. B. Salamon, Shantanu Sinha, J. J. Rhyne, J. E. Cunningham, Ross W. Erwin, Julie Borchers, and C. P. Flynn, Phys. Rev. Lett. **56**, 259 - 262 (1986)

- Observation of a Magnetic Antiphase Domain Structure with Long- Range Order in a Synthetic Gd-Y Superlattice

C. F. Majkrzak, J. W. Cable, J. Kwo, M. Hong, D. B. McWhan, Y. Yafet, and J. V. Waszczak,C. Vettier, Phys. Rev. Lett. **56**, 2700 - 2703 (1986)

- Layered Magnetic Structures: Evidence for Antiferromagnetic Coupling of Fe Layers across Cr Interlayers

P. Grünberg, R. Schreiber, Y. Pang, M. B. Brodsky, and H. Sowers, Phys. Rev. Lett. **57**, 2442 - 2445 (1986)

Magnetic coupling in multilayers

- Long-range incommensurate magnetic order in a Dy-Y multilayer

M. B. Salamon, Shantanu Sinha, J. J. Rhyne, J. E. Cunningham, Ross W. Erwin, Julie Borchers, and C. P. Flynn, Phys. Rev. Lett. 56, 259 - 262 (1986)

- Observation of a Magnetic Antiphase Domain Structure with Long-Range Order in a Synthetic Gd-Y Superlattice

C. F. Majkrzak, J. W. Cable, J. Kwo, M. Hong, D. B. McWhan, Y. Yafet, and J. V. Waszczak,C. Vettier, Phys. Rev. Lett. 56, 2700 - 2703 (1986)

- Layered Magnetic Structures: Evidence for Antiferromagnetic Coupling of Fe Layers across Cr Interlayers

P. Grünberg, R. Schreiber, Y. Pang, M. B. Brodsky, and H. Sowers, Phys. Rev. Lett. 57, 2442 - 2445 (1986)

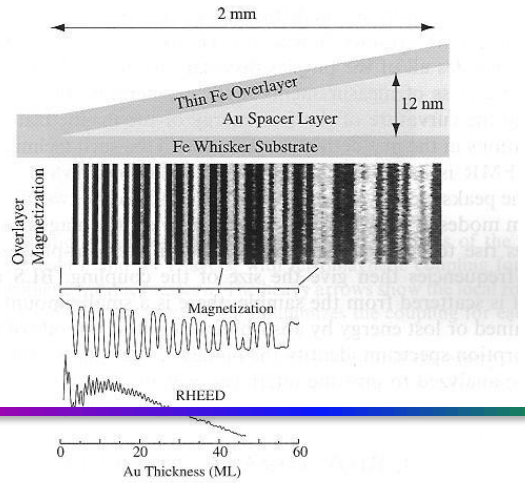

Coupling in wedge-shaped
Fe/Cr/Fe
Fe/Au/Fe
Fe/Ag/Fe
J. Unguris, R. J. Celotta, and D. T. Pierce

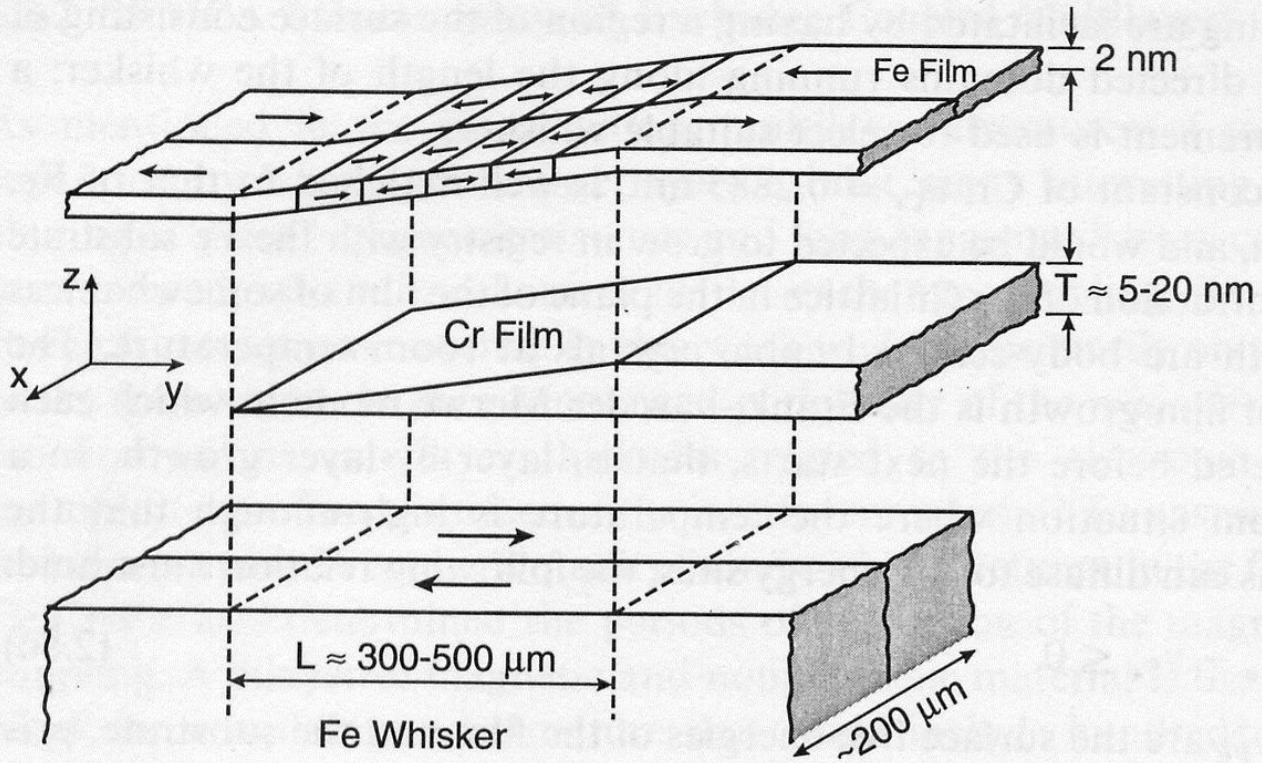

Fig. 2.41. A schematic expanded view of the sample structure showing the Fe(0 0 1) single-crystal whisker substrate, the evaporated Cr wedge, and the Fe overlayer. The arrows in the Fe show the magnetization direction in each domain. The *z*-scale is expanded approximately 5000 times. (From [2.206])

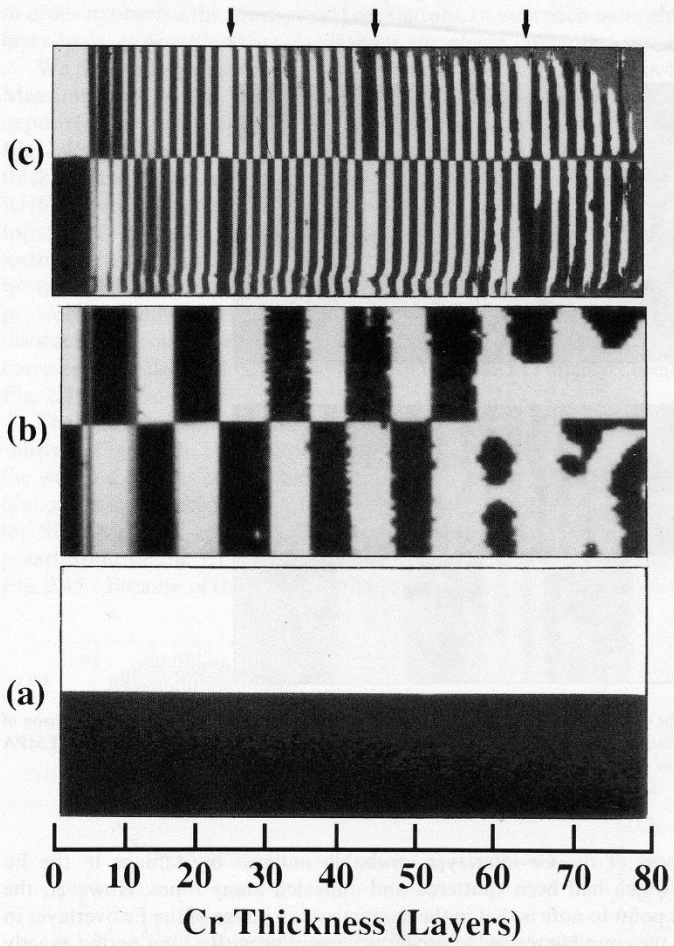

Fig. 2.43. SEMPA image of the magnetization M_y (axes as in Fig. 2.41) showing domains in (**a**) the clean Fe whisker, (**b**) the Fe layer covering the Cr spacer layer evaporated at 30 °C, and (**c**) the Fe layer covering a Cr spacer evaporated on the Fe whisker held at 350 °C. The scale at the bottom shows the increase in the thickness of the Cr wedge in (**b**) and (**c**). The arrows at the top of (**c**) indicate the Cr thicknesses where there are phase slips. The region of the whisker imaged is about 0.5 mm long

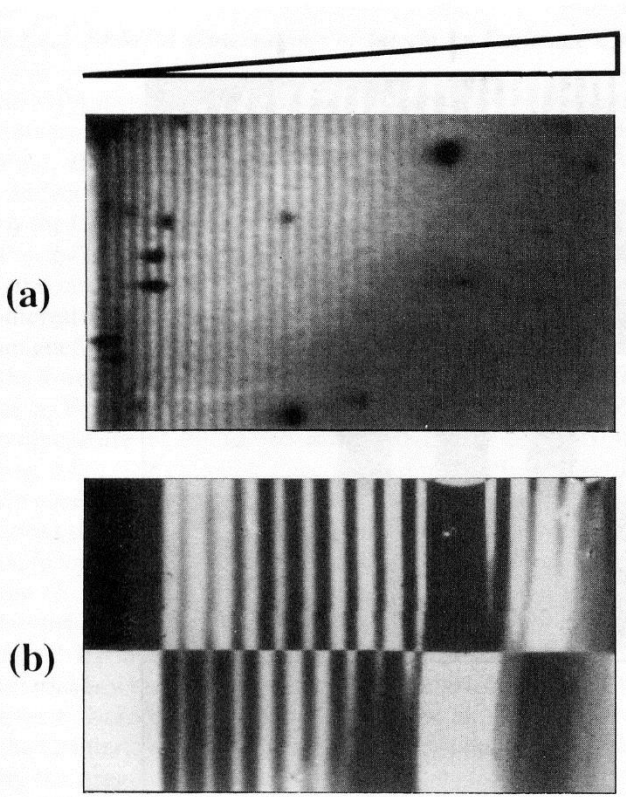

Fig. 2.44. The effect of roughness on the inertlayer exchange coupling is shown by a comparison of (**a**) the oscillations of the RHEED intensity along the bare Cr wedge with (**b**) the SEMPA magnetization image over the same part of the wedge

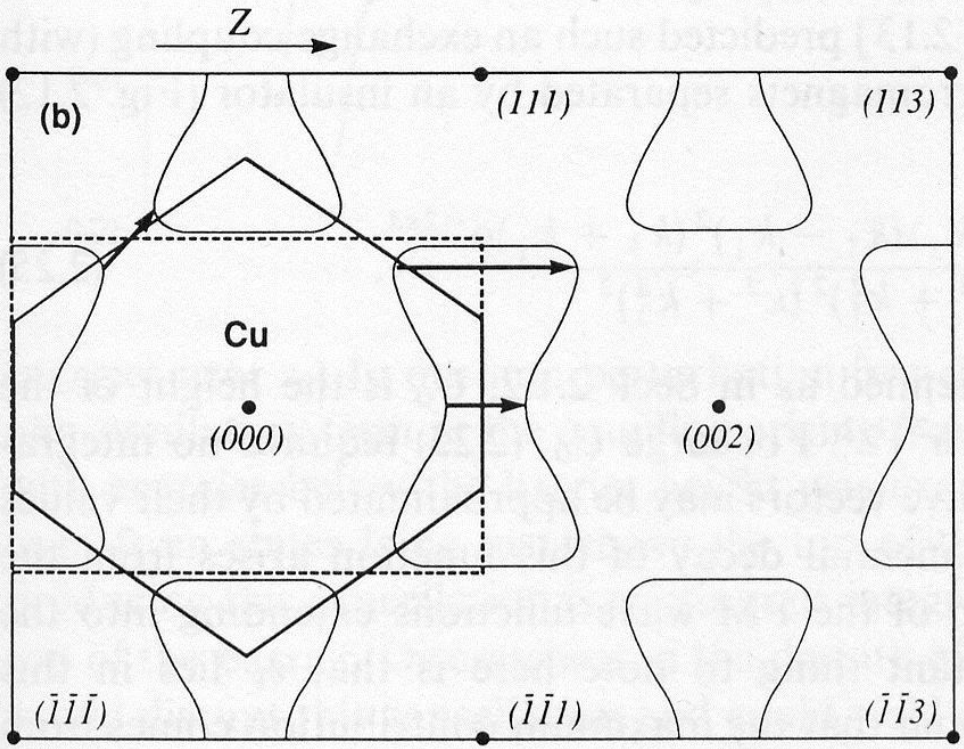

Fig. 2.11. Fermi surface of Cu in the (1 0 0) plane in the extended zone scheme. Arrows indicate values of $2(k_F - G)$ for reciprocal lattice vectors G which can give rise to oscillations with periods greater than π/k_F

Oscillatory magnetic coupling in multilayers

Ru interlayer has the largest coupling strength

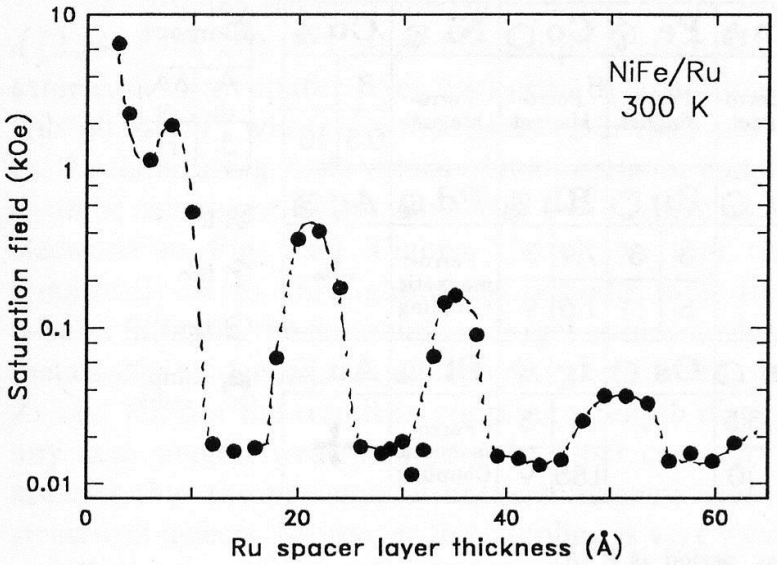

Fig. 2.58. Dependence of saturation field on Ru spacer layer thickness for several series of $Ni_{81}Fe_{19}$/Ru multilayers with structure, 100 Å Ru/[30 Å $Ni_{81}Fe_{19}$/Ru(t_{Ru})]$_{20}$, where the topmost Ru layer thickness is adjusted to be $\simeq$25 Å for all samples

	$\|J_1\|$ at 1st peak (erg/cm^2)	Period (nm)
Cu	0.3	1
V	0.1	0.9
Cr	0.24	1.8
Ir	0.81	0.9
Ru	5.0	1.2

S. S. P. Parkin

Kwo et al, PRB **35** 7295 (1987)
Modulated magnetic properties in synthetic rare-earth Gd-Y superlattices

Spin-dependent conduction in Ferromagnetic metals (Two-current model)

First suggested by Mott (1936)

Experimentally confirmed by I. A. Campbell and A. Fert (~1970)

At low temperature

$$\rho = \frac{\rho_\uparrow \rho_\downarrow}{\rho_\uparrow + \rho_\downarrow}$$

At high temperature

$$\rho = \frac{\rho_\uparrow \rho_\downarrow + \rho_{\uparrow\downarrow}(\rho_\uparrow + \rho_\downarrow)}{\rho_\uparrow + \rho_\downarrow + 4\rho_{\uparrow\downarrow}}$$

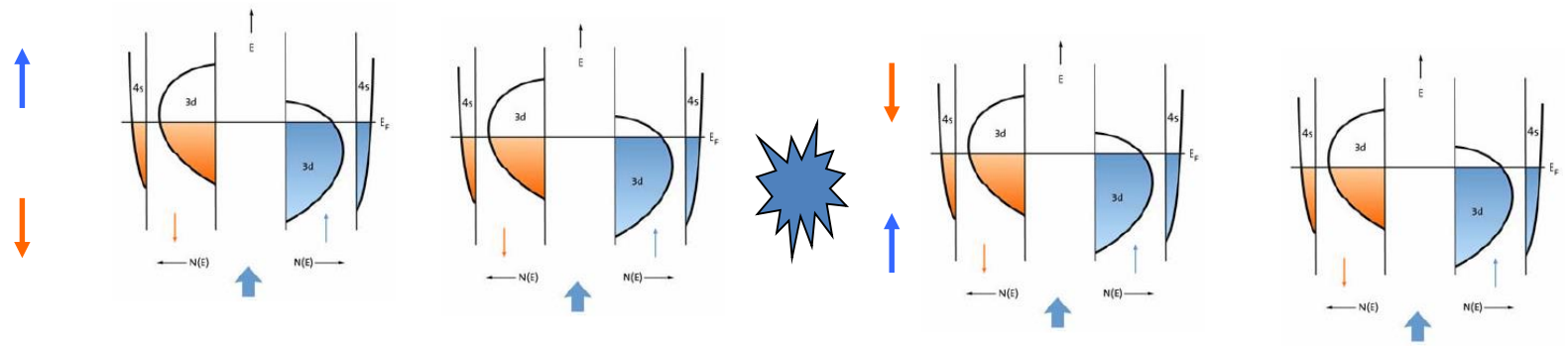

Spin mixing effect equalizes two currents

Two Current Model

s electrons carry the electric current

resistivity (spin-dependent s → d scattering)

$$R^{s} = \text{const. } N_d^{s}$$

number of empty *d* states

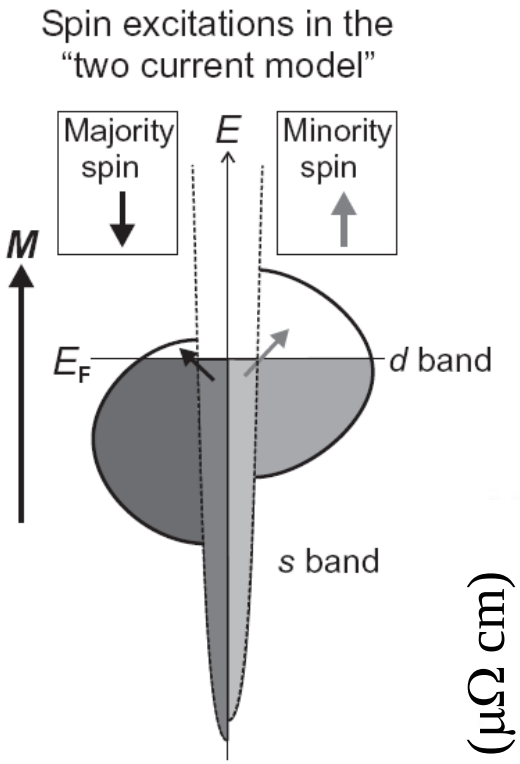

spin selective scattering

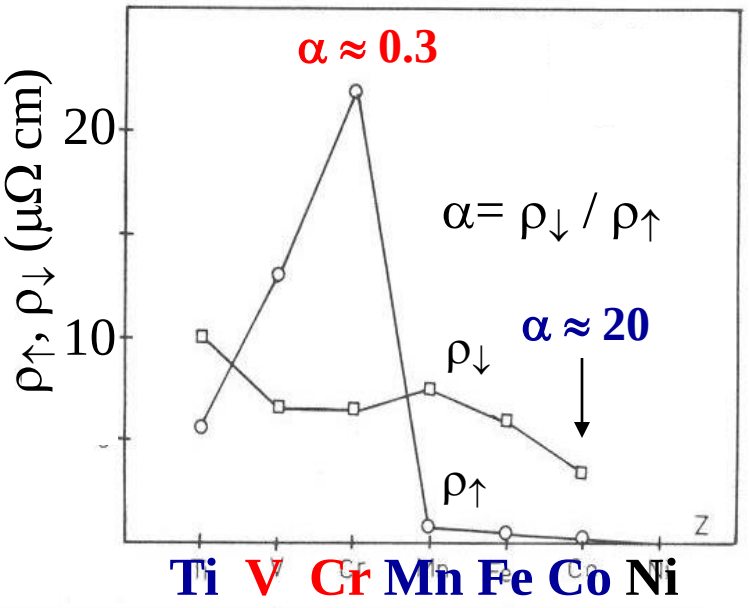

element	$N_h^{d\ a}$	$\lvert m \rvert$ [μ_B]	$R^{\ b}$ [Ω m]
Fe (bcc)	3.90	2.216	9.71×10^{-8}
Co (hcp)	2.80	1.715	6.25×10^{-8}
Ni (fcc)	1.75	0.616	6.84×10^{-8}
Cu (fcc)	0.50	–	1.68×10^{-8}

A. Fert, I.A. Campbell, PRL **21**, 1190 (1968)

Anisotropic magnetoresistance (AMR)

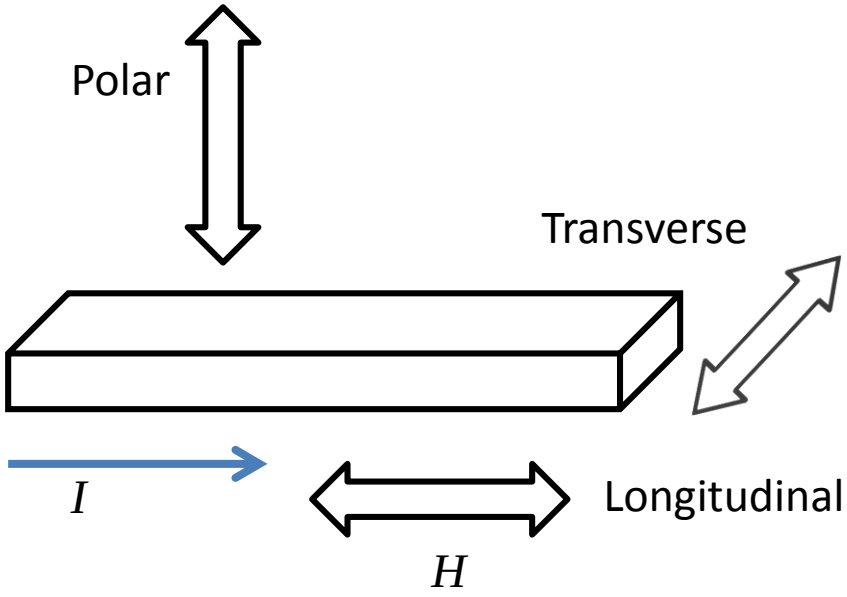

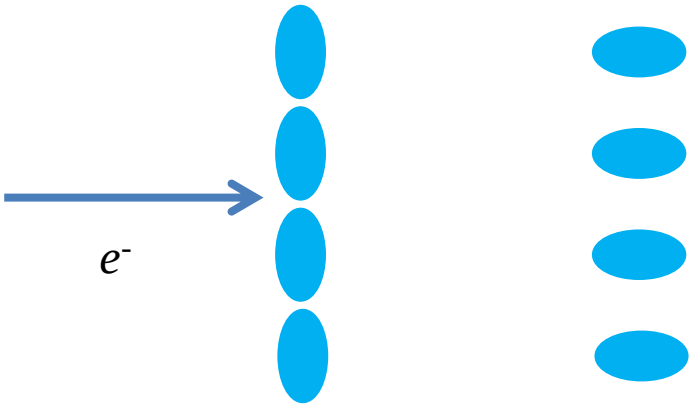

$R_{Long.} > R_{Trans.}, R_{Pol.}$

Geometrical size effect

Fe 100nm 10K

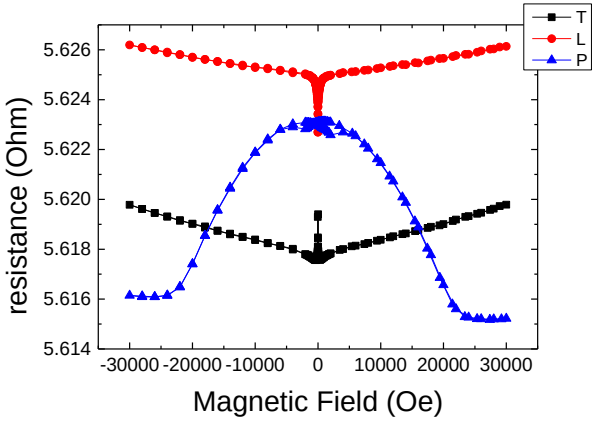

Ni 100nm 10K

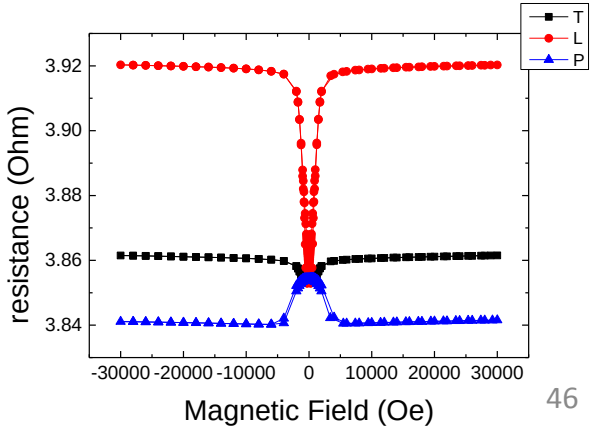

outline

- Giant Magnetoresistance, Tunneling Magnetoresistance
- Spin Transfer Torque
- Pure Spin current (no net charge current)
  - Spin Hall, Inverse Spin Hall effects
  - Spin Pumping effect
  - Spin Seebeck effect
- Micro and nano Magnetics

2007 Nobel prize in Physics

2007年諾貝爾物理獎得主 左 亞伯・費爾(Albert Fert) 與右彼得・葛倫貝格(Peter Grünberg)

(圖片資料來源：Copyright © Nobel Web AB 2007/ Photo: Hans Mehlin)

Giant Magnetoresistance
Tunneling Magnetoresistance

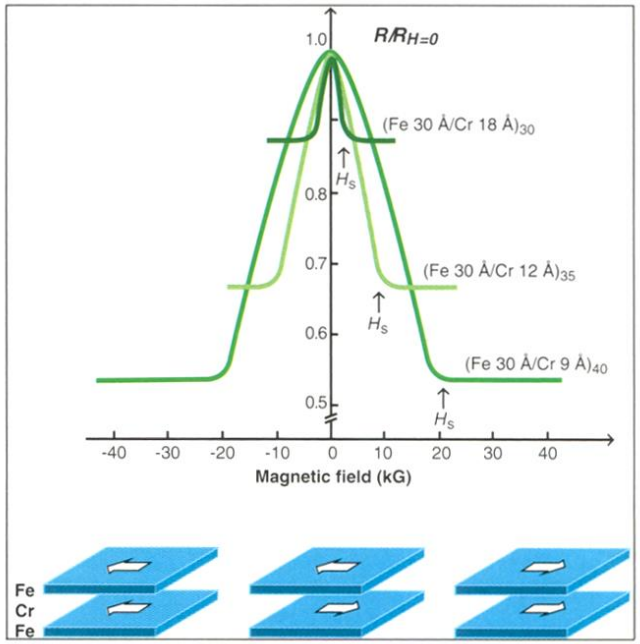

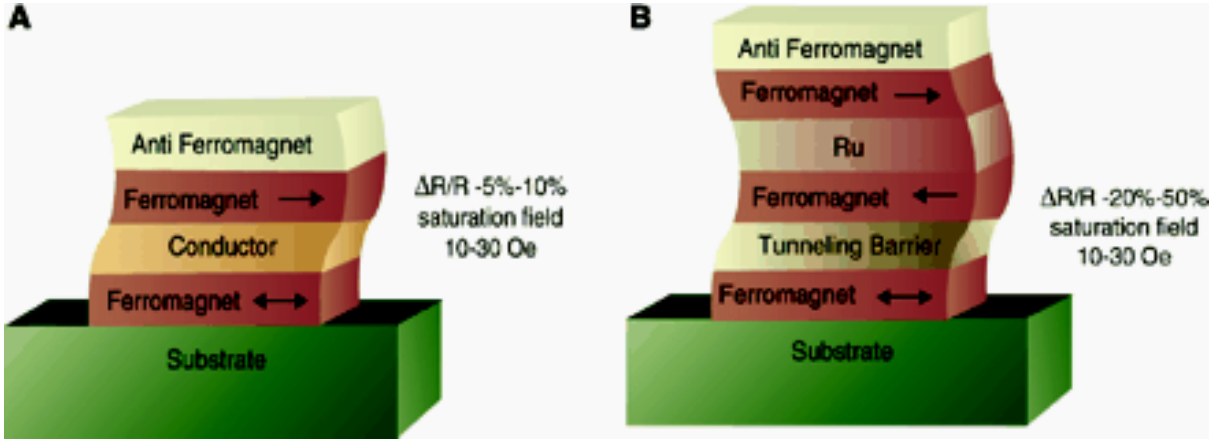

Discovery of Giant MR -- Two-current model combines with magnetic coupling in multilayers

Spin-dependent transport structures. (A) Spin valve. (B) Magnetic tunnel junction. (from Science)

Moodera's group, PRL **74**, 3273 (1995)

Fert's group, PRL **61**, 2472 (1988)

Miyazaki's group, JMMM **139**, L231(1995)

Spin valve –

a sandwich structure
with a free ferromagnetic layer (F) and a fixed F layer
pinned by an antiferromagnetic (AF) layer

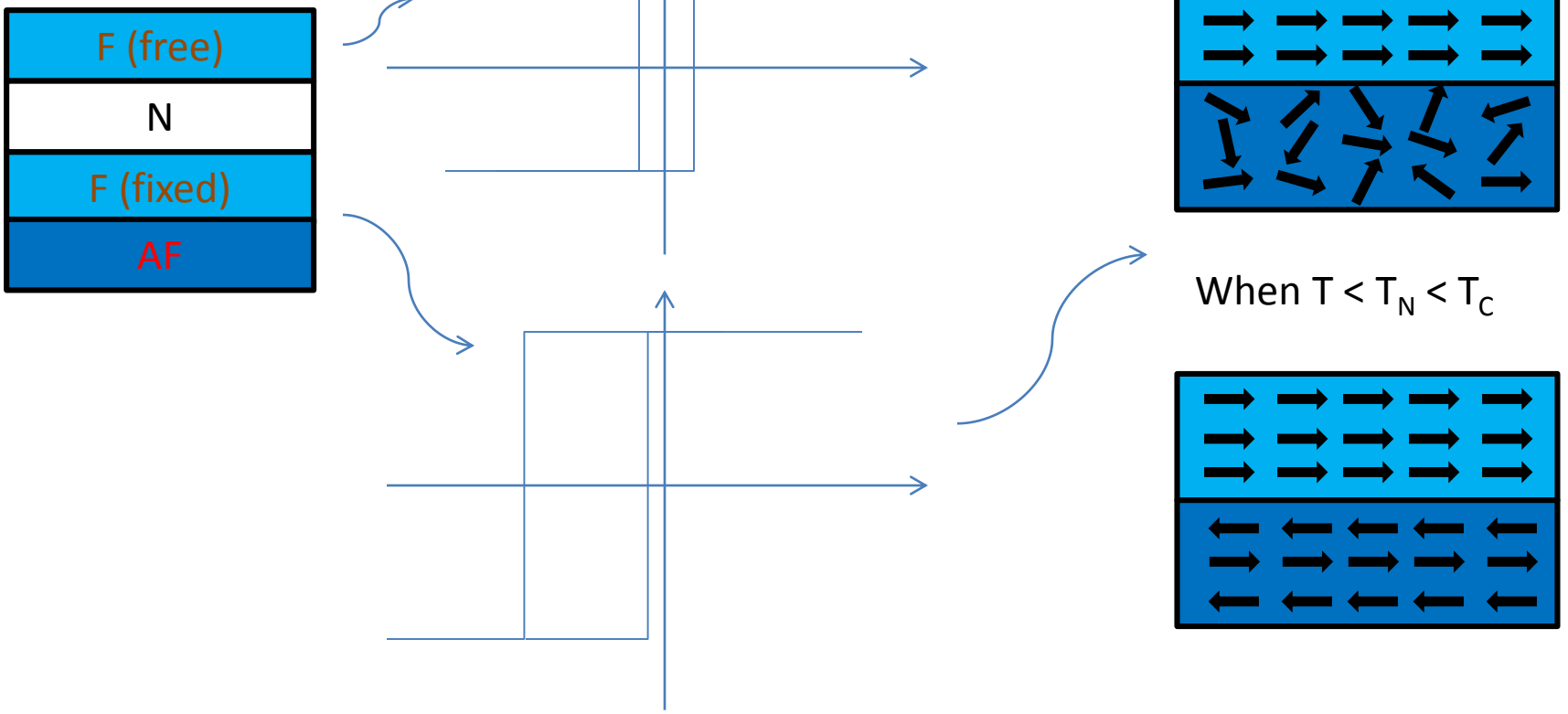

Transport geometry

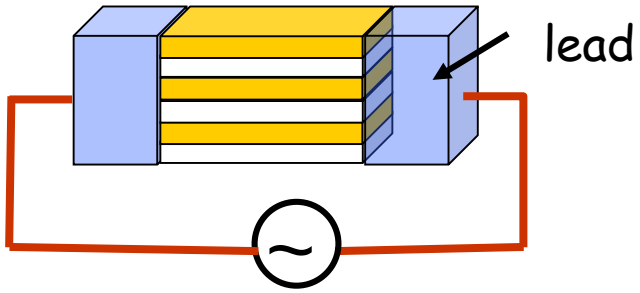

CIP geometry

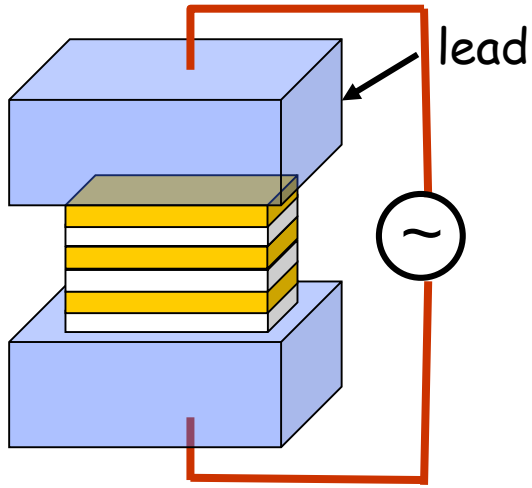

CPP geometry

- In metallic multilayers, CIP resistance can be measured easily, CPP resistance needs special techniques.
- From CPP resistance in metallic multilayers, one can measure interface resistances, spin diffusion lengths, and polarization in ferromagnetic materials, etc.
- CPP magnetoresistance of magnetic multilayers: A critical review

  Jack Bass

  Journal of Magnetism and Magnetic Materials 408 (2016) 244–320

Valet and Fert model of (CPP-)GMR

Based on the Boltzmann equation

A semi-classical model with spin taken into consideration

$$j_{+(-)} = \frac{1}{e\rho_{+(-)}} \frac{\partial \mu_{+(-)}}{\partial x}$$

$$j_+ + j_- = j_e$$

$$\frac{\partial (j_+ - j_-)}{\partial x} = \frac{2eN(E_F)\Delta\mu}{\tau_{sf}}$$

$$\frac{\partial^2 \mu_{+(-)}}{\partial z^2} = \frac{\mu_{+(-)}}{l_{sf}^2}$$

$$l_{sf}^F = \left[\lambda_{sf}^F / 3(\lambda_\uparrow^{-1} + \lambda_\downarrow^{-1})\right]^{1/2}, \quad l_{sf}^N = \left[\lambda_{sf}^N \lambda / 6\right]^{1/2}$$

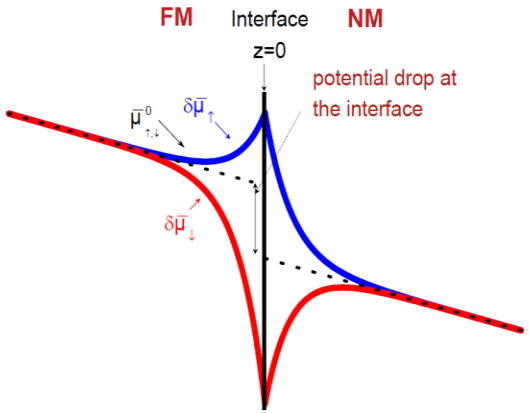

$\Delta\mu$ for antiparallel aligned multilayers

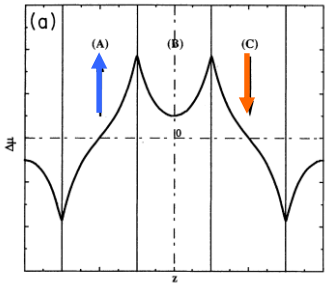

$\Delta\mu$ for parallel aligned multilayers

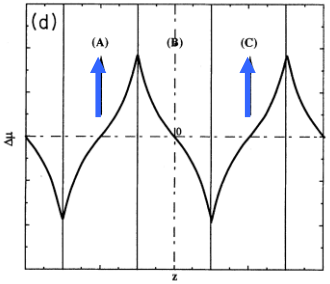

Spin imbalance induced charge accumulation at the interface is important

Spin diffusion length, instead of mean free path, is the dominant physical length scale

Spin Diffusion: The Johnson Transistor
non-local measurement

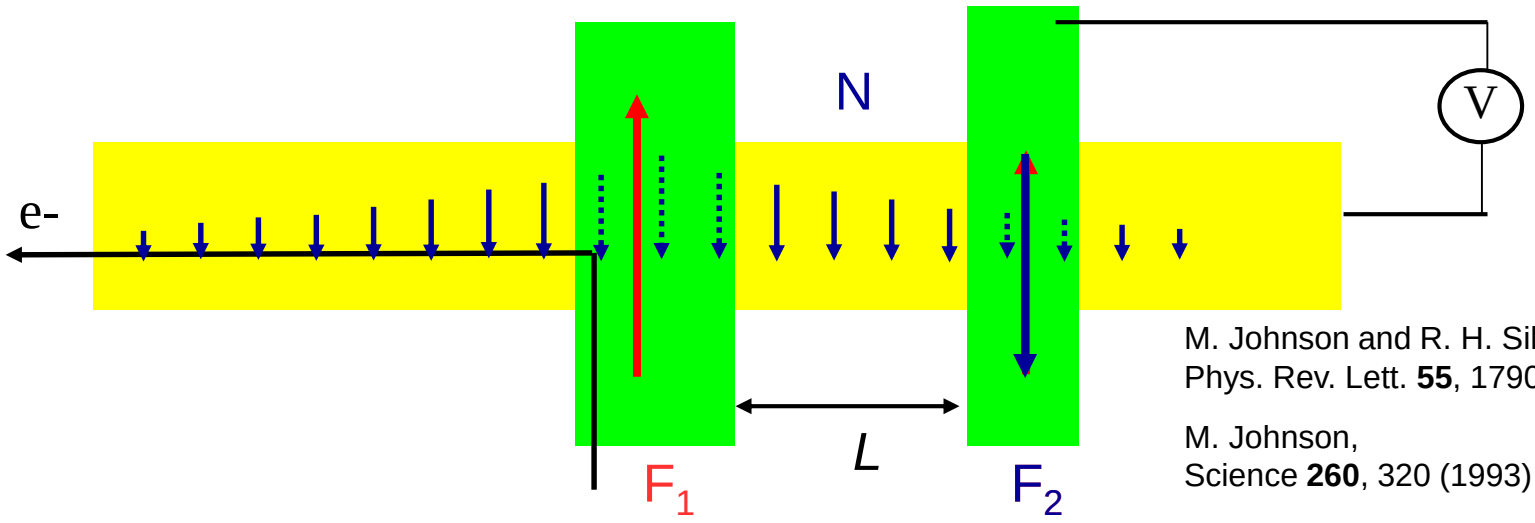

M. Johnson and R. H. Silsbee, Phys. Rev. Lett. **55**, 1790 (1985)

M. Johnson, Science **260**, 320 (1993)

First Experimental Demonstrations

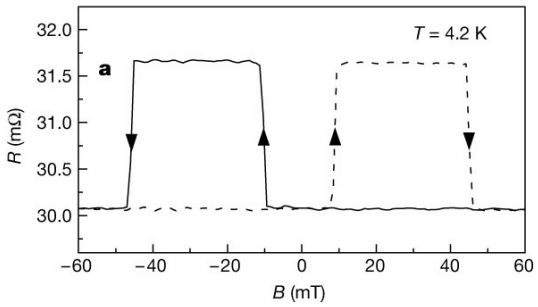

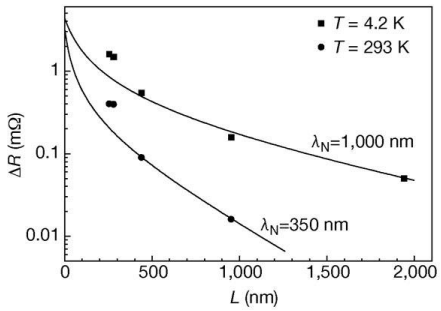

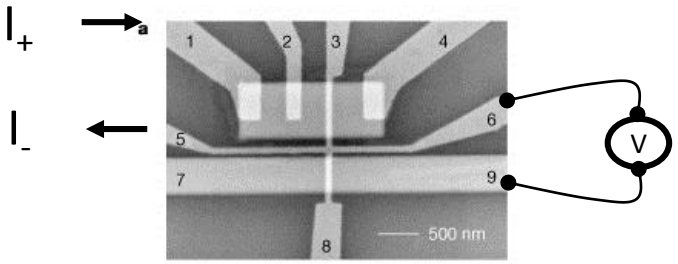

Cu film: λ_s = 1 μm (4.2 K)

Jedema *et al.*, Nature **410**, 345 (2001)

outline

- Giant Magnetoresistance, Tunneling Magnetoresistance
- Spin Transfer Torque
- Pure Spin current (no net charge current)
  - Spin Hall, Inverse Spin Hall effects
  - Spin Pumping effect
  - Spin Seebeck effect
- Micro and nano Magnetics

Spin Transfer Torque

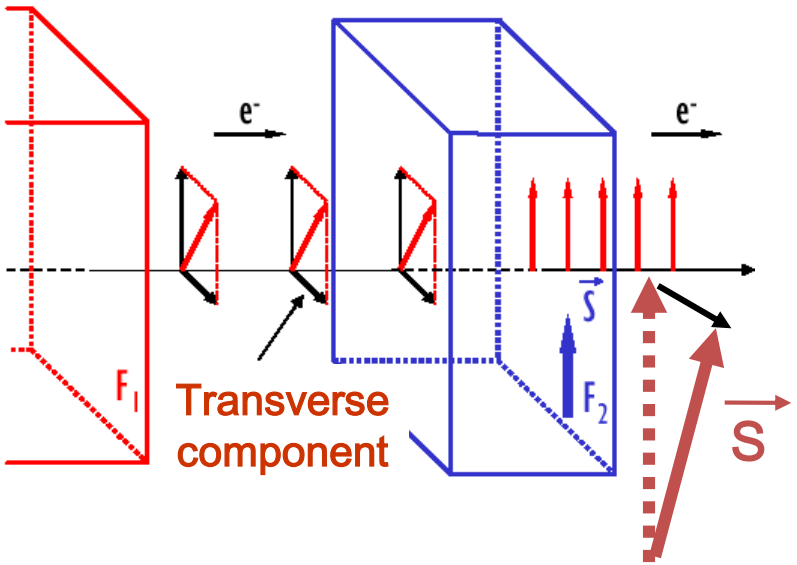

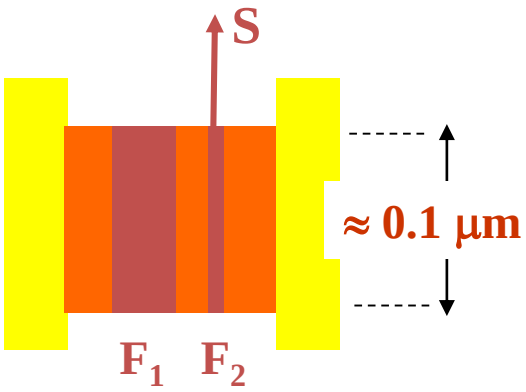

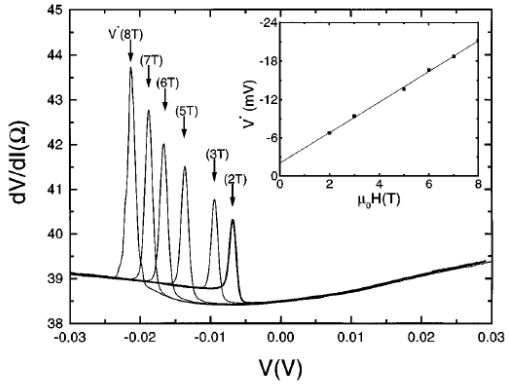

FIG. 1. The point contact $dV/dI(V)$ spectra for a series of magnetic fields (2, 3, 5, 6, 7, and 8 T) revealing an upward step and a corresponding peak in dV/dI at a certain negative bias voltage $V^*(H)$. The inset shows that $V^*(H)$ increases linearly with the applied magnetic field H.

Tsoi et al. PRL **61**, 2472 (1998)

The transverse spin component is lost by the conduction electrons, transferred to the global spin of the layer $\vec{S}$

$$\dot{\boldsymbol{S}}_{1,2} = \left(I_e\, g/e\right)\hat{\boldsymbol{s}}_{1,2} \times \left(\hat{\boldsymbol{s}}_1 \times \hat{\boldsymbol{s}}_2\right)$$

Slonczewski JMMM **159**, L1 (1996)

Modified Landau-Lifshitz-Gilbert (LLG) equation

$$\frac{dm}{dt} = -\gamma m \times H_{eff} + \alpha m \times \frac{dm}{dt} + \frac{\gamma \hbar P I}{2e\mu_0 M_S V}(m \times \sigma \times m)$$

Experimantally determined current density ~10^{10}-10^{12}A/m^2

Spin Transfer Torque

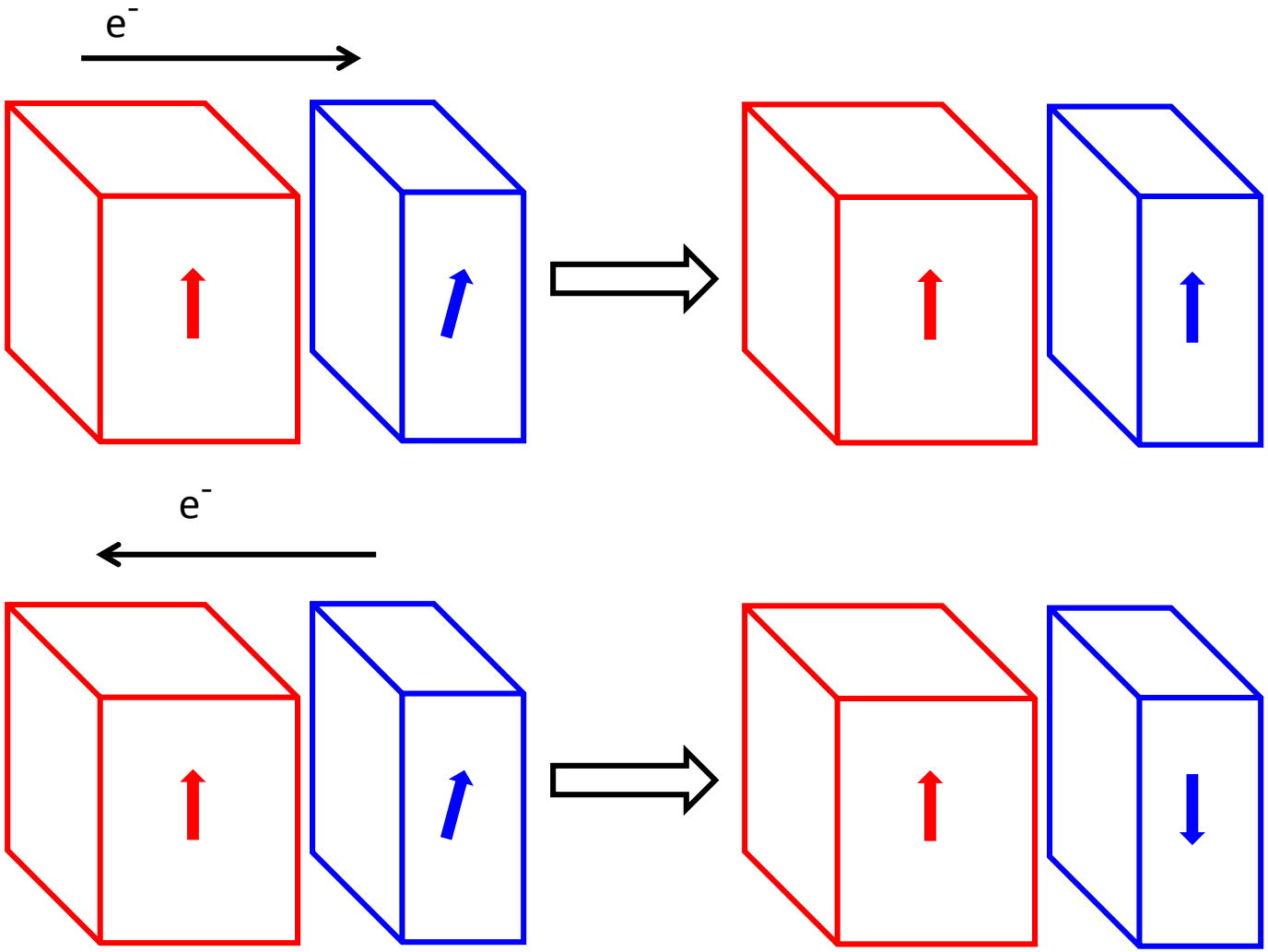

In a trilayer, current direction determines the relative orientation of F_1 and F_2

Spin Transfer Torque

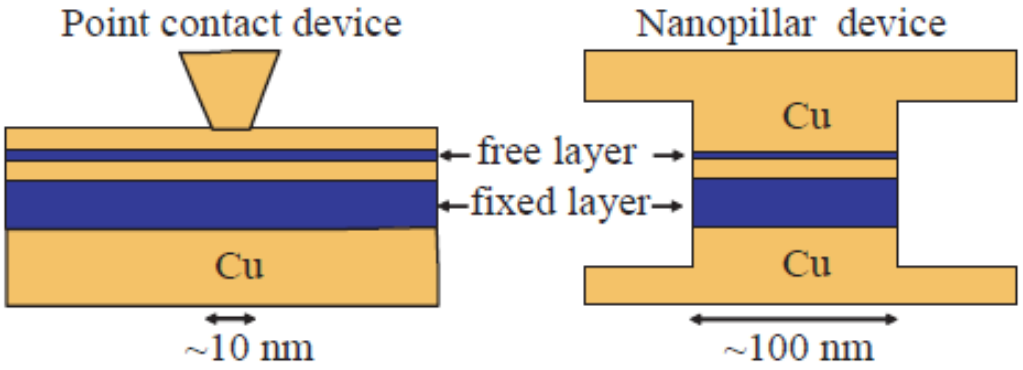

Ralph and Stiles "Spin transfer torques". *JMMM* **320,** 1190–1216 (2008).

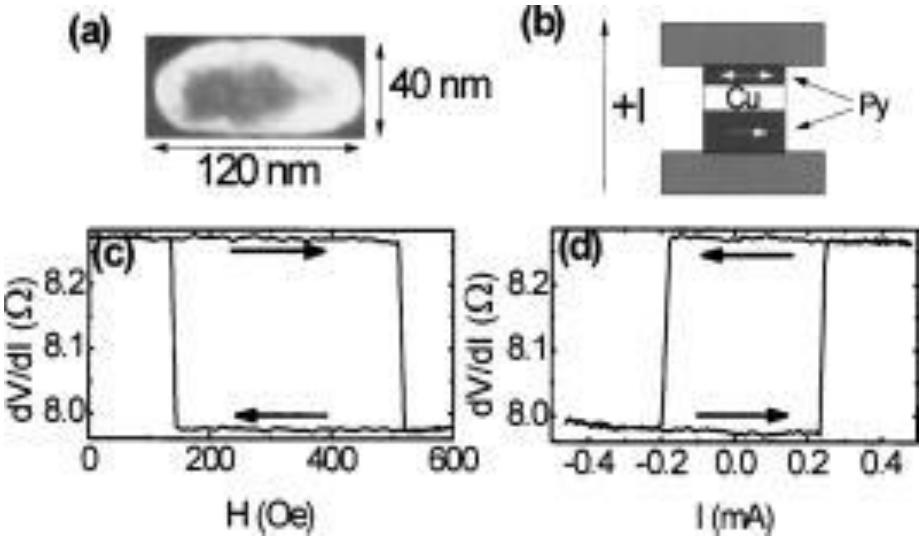

(c) Minor loop of free layer and
(d) spin transfer curve at 293*K*
120 Cu/20 Py/12 Cu/X Py/2 Cu/30 Au

Ralph and Buhrman's group, APL **87**, 112507 (2005)

Spin Transfer Torque

Landau-Lifshitz-Gilbert equation with Spin Transfer Torque terms

Current induced domain wall motion

Passing spin polarized current from Domain A to Domain B⇒B switches

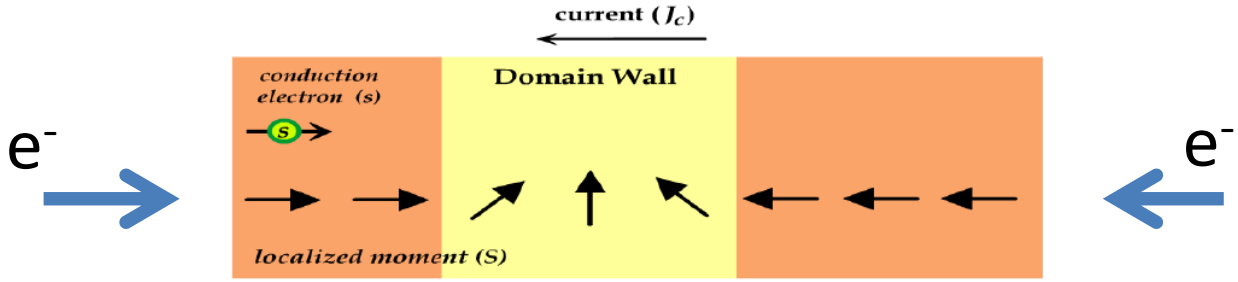

Domain A **Domain B**

$$\frac{\partial \vec{M}}{\partial t} = -\gamma \vec{M} \times \vec{H}_{eff} + \frac{\alpha}{M_s} \vec{M} \times \frac{\partial \vec{M}}{\partial t} + \vec{\mathrm{T}}_{STT}$$

Berger, *JAP* **55**, 1954 (1984)
Tatara *et. al.*, *PRL* **92**, 086601 (2004)
Zhang *et. al.*, *PRL* **93**, 127204 (2004)
Thiaville *et. al.*, *Europhys. Lett*. **69**, 990 (2005)
Stiles *et. al.*, *PRB* **75**, 214423 (2007)

Spin Transfer Torque

Landau-Lifshitz-Gilbert equation with Spin Transfer Torque terms

$$\frac{\partial \vec{M}}{\partial t} = -\gamma \vec{M} \times \vec{H}_{\text{eff}} + \frac{\alpha}{M_s} \vec{M} \times \frac{\partial \vec{M}}{\partial t} - \frac{b_j}{M_s^2} \vec{M} \times \left(\vec{M} \times \frac{\partial \vec{M}}{\partial x}\right) - \frac{c_j}{M_s} \vec{M} \times \frac{\partial \vec{M}}{\partial x}$$

$b_j, c_j \sim JP/t$

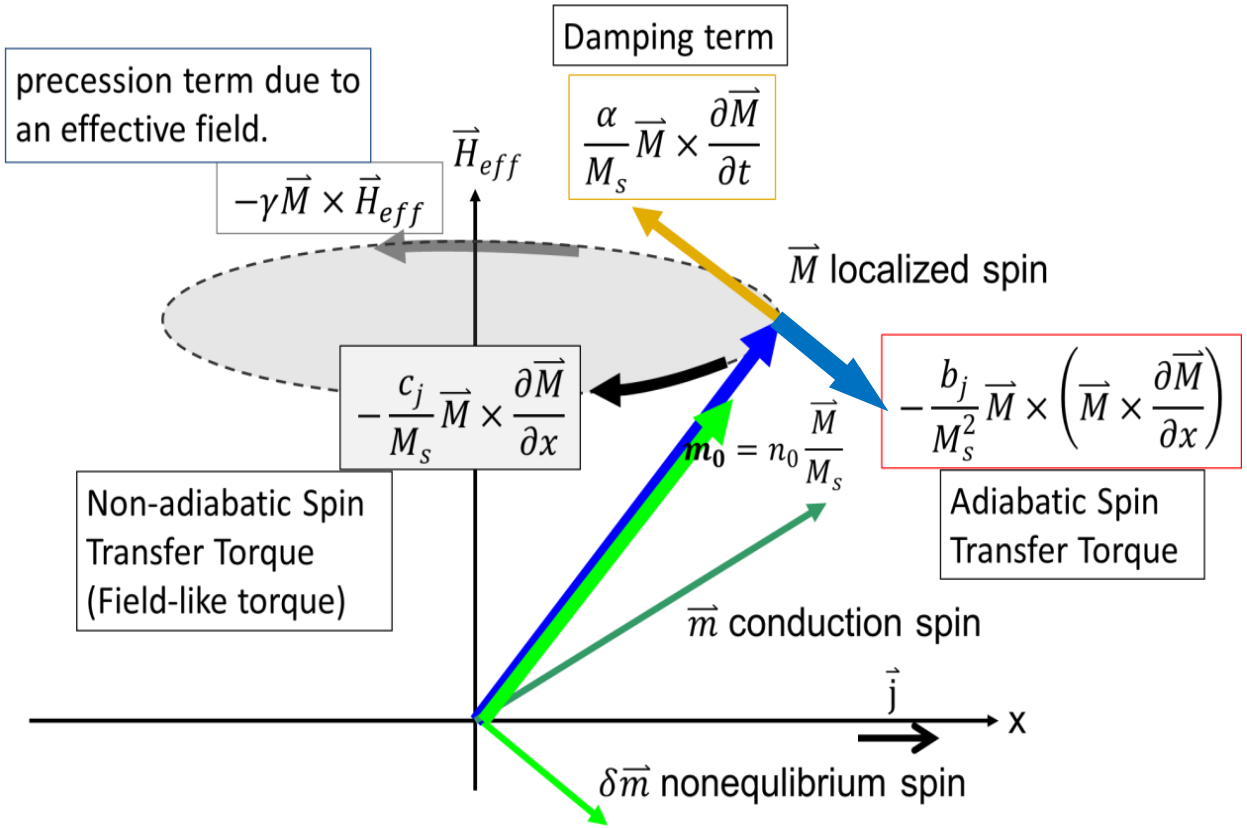

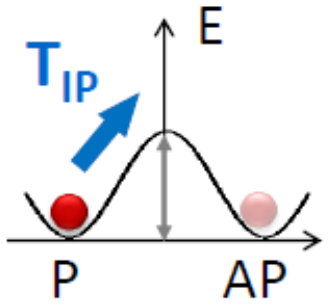

In-plane torque
Anti-damping
Destabilizes M

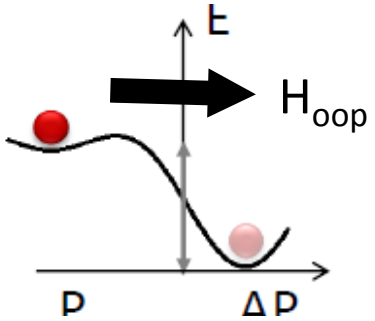

Out-of-plane torque
Field-like torque
Modifies energy barrier